The Astrophysical Journal, 767:57 (28pp), 2013 April 10 doi:10.1088/0004-637X/767/1/57


# TYPE Iax SUPERNOVAE: A NEW CLASS OF STELLAR EXPLOSION*

Ryan J. Foley[1,12], P. J. Challis[1], R. Chornock[1], M. Ganeshalingam[2], W. Li[2,13], G. H. Marion[1], N. I. Morrell[3], G. Pignata[4], M. D. Stritzinger[5], J. M. Silverman[2,6], X. Wang[7], J. P. Anderson[8], A. V. Filippenko[2], W. L. Freedman[9], M. Hamuy[8], S. W. Jha[10], R. P. Kirshner[1], C. McCully[10], S. E. Persson[9], M. M. Phillips[3], D. E. Reichart[11], and A. M. Soderberg[1]

[1] Harvard-Smithsonian Center for Astrophysics, 60 Garden Street, Cambridge, MA 02138, USA; rfoley@cfa.harvard.edu
[2] Department of Astronomy, University of California, Berkeley, CA 94720-3411, USA
[3] Carnegie Observatories, Las Campanas Observatory, La Serena, Chile
[4] Departamento de Ciencias Fisicas, Universidad Andres Bello, Avda. Republica 252, Santiago, Chile
[5] Department of Physics and Astronomy, Aarhus University, Ny Munkegade, DK-8000 Aarhus C, Denmark
[6] Department of Astronomy, University of Texas, Austin, TX 78712-0259, USA
[7] Physics Department and Tsinghua Center for Astrophysics (THCA), Tsinghua University, Beijing 100084, China
[8] Departamento de Astronomía, Universidad de Chile, Casilla 36-D, Santiago, Chile
[9] Observatories of the Carnegie Institution of Washington, 813 Santa Barbara St., Pasadena, CA 91101, USA
[10] Department of Physics and Astronomy, Rutgers, the State University of New Jersey, 136 Frelinghuysen Road, Piscataway, NJ 08854, USA
[11] Department of Physics and Astronomy, University of North Carolina at Chapel Hill, Chapel Hill, NC, USA
*Received 2012 December 3; accepted 2013 February 1; published 2013 March 25*

## ABSTRACT

We describe observed properties of the Type Iax class of supernovae (SNe Iax), consisting of SNe observationally similar to its prototypical member, SN 2002cx. The class currently has 25 members, and we present optical photometry and/or optical spectroscopy for most of them. SNe Iax are spectroscopically similar to SNe Ia, but have lower maximum-light velocities ($2000 \lesssim |v| \lesssim 8000$ km s$^{-1}$), typically lower peak magnitudes ($-14.2 \geqslant M_{V,\mathrm{peak}} \gtrsim -18.9$ mag), and most have hot photospheres. Relative to SNe Ia, SNe Iax have low luminosities for their light-curve shape. There is a correlation between luminosity and light-curve shape, similar to that of SNe Ia, but offset from that of SNe Ia and with larger scatter. Despite a host-galaxy morphology distribution that is highly skewed to late-type galaxies without any SNe Iax discovered in elliptical galaxies, there are several indications that the progenitor stars are white dwarfs (WDs): evidence of C/O burning in their maximum-light spectra, low (typically $\sim$0.5 $M_\odot$) ejecta masses, strong Fe lines in their late-time spectra, a lack of X-ray detections, and deep limits on massive stars and star formation at the SN sites. However, two SNe Iax show strong He lines in their spectra. The progenitor system and explosion model that best fits all of the data is a binary system of a C/O WD that accretes matter from a He star and has a deflagration. At least some of the time, this explosion will not disrupt the WD. The small number of SNe in this class prohibit a detailed analysis of the homogeneity and heterogeneity of the entire class. We estimate that in a given volume there are $31^{+17}_{-13}$ SNe Iax for every 100 SNe Ia, and for every 1 $M_\odot$ of iron generated by SNe Ia at $z = 0$, SNe Iax generate $\sim$0.036 $M_\odot$. Being the largest class of peculiar SNe, thousands of SNe Iax will be discovered by LSST. Future detailed observations of SNe Iax should further our understanding of both their progenitor systems and explosions as well as those of SNe Ia.

*Key words:* supernovae: general – supernovae: individual (SN 1991bj, SN 1999ax, SN 2002bp, SN 2002cx, SN 2003gq, SN 2004cs, SN 2004gw, SN 2005P, SN 2005cc, SN 2005hk, SN 2006hn, SN 2007J, SN 2007ie, SN 2007qd, SN 2008A, SN 2008ae, SN 2008ge, SN 2008ha, SN 2009J, SN 2009ku, SN 2010ae, SN 2010el, SN 2011ay, SN 2011ce, SN 2012Z)

*Online-only material:* color figures, extended figure

## 1. INTRODUCTION

Most thermonuclear supernovae are spectroscopically defined as Type Ia. These supernovae (SNe) lack hydrogen and helium in their spectra (except perhaps from circumstellar interaction), and most have strong lines from intermediate mass elements (IMEs) in their near-maximum-light spectra (see Filippenko 1997 for a review of SN classification). The bulk of observational diversity within this group can be described by a single parameter that relates peak luminosity with light-curve shape (a width–luminosity relation or WLR; Phillips 1993), intrinsic color (Riess et al. 1996), and $^{56}$Ni mass (Mazzali et al. 2007). However, there is additional diversity related to ejecta velocity (e.g., Benetti et al. 2005; Foley & Kasen 2011; Ganeshalingam et al. 2011). The ability to collapse the observational diversity of this class to one or two parameters suggests that most SNe Ia have similar progenitor stars (although not necessarily progenitor systems, as some SN Ia observables correlate with their progenitor environment; Foley et al. 2012b) and explosion mechanisms. There are also examples of particular thermonuclear SNe that do not follow this parameterization (e.g., Li et al. 2001a; Howell et al. 2006; Foley et al. 2010b; Ganeshalingam et al. 2012), which may be the result of these SNe having different progenitors and/or explosion mechanisms than most SNe Ia, rather than being extreme examples of the normal SN Ia progenitor system and explosion mechanism.

Almost all thermonuclear SNe that are outliers to the trends defined by SNe Ia are part of a single, relatively large class. Members of this class, previously labeled "SN 2002cx-like"

* This paper is dedicated to the memory of our friend and colleague, Dr. Weidong Li, a pioneer in the identification and detailed study of this class of objects.
[12] Clay Fellow.
[13] Deceased 2011 December 12.

after the prototypical object (Li et al. 2003), have peak magnitudes $\gtrsim$1 mag below that of normal SNe Ia, spectra that show low-velocity ejecta, and maximum-light spectra that typically resemble those of the high-luminosity SN Ia 1991T (blue continua and absorption from higher-ionization species consistent with a hot photosphere). Studying thermonuclear outliers can both help determine what progenitors and explosion mechanisms do *not* produce normal SNe Ia and constrain various models by examining the extremes of the population.

In addition to the properties mentioned above, the SN 2002cx-like class has several observational properties that distinguish it from that of normal SNe Ia: low luminosity for its light-curve shape (e.g., Li et al. 2003); no observed second maximum in the near-infrared (NIR) bands (e.g., Li et al. 2003); late-time spectra dominated by narrow permitted Fe II lines (Jha et al. 2006; Sahu et al. 2008), but can occasionally have strong [Fe II] emission (Foley et al. 2010c); strong mixing of the ejecta (Jha et al. 2006; Phillips et al. 2007); and a host-galaxy morphology distribution highly skewed to late-type galaxies, and no member of this class has been discovered in an elliptical galaxy (Foley et al. 2009; Valenti et al. 2009). Additionally, some members of the class, such as SN 2007J, display strong He I lines in their spectra (Foley et al. 2009).

Because of these physical distinctions as well as others discussed in this paper, we designate this class of objects "Type Iax supernovae" or SNe Iax. This designation indicates the observational and physical similarities to SNe Ia, but also emphasizes the physical differences between SNe Iax and normal SNe Ia (e.g., SNe Iax are not simply a subclass of SNe Ia) and will hopefully reduce confusion within the literature.

Several of the extreme characteristics of some members of this class, including low kinetic energy and significant mixing in the ejecta, may be consistent with a full deflagration of a white dwarf (WD; Branch et al. 2004; Phillips et al. 2007), rather than a deflagration that transitions into a detonation as expected for normal SNe Ia (Khokhlov 1991). Because of their low velocities, which eases line identification and helps probe the deflagration process, which is essential to all SN Ia explosions, this class is particularly useful for understanding typical SN Ia explosions.

An extreme member of this class, SN 2008ha (Foley et al. 2009; Valenti et al. 2009; Foley et al. 2010a), was much fainter (peaking at $M_V = -14.2$ mag) and had a significantly lower velocity ($|v| \approx 2000$ km s$^{-1}$) than the typical member. Although its maximum-light spectrum indicates that the object underwent C/O burning (Foley et al. 2010a), certain observations are consistent with a massive-star progenitor (Foley et al. 2009; Valenti et al. 2009; Moriya et al. 2010). Nonetheless, a massive-star progenitor is inconsistent with other observables (Foley et al. 2010a). SN 2008ha generated $\sim 10^{-3}\ M_\odot$ of $^{56}$Ni and ejected $\sim 0.3\ M_\odot$ of material (Foley et al. 2010a), suggesting that the most plausible explanation was a failed deflagration of a WD (Foley et al. 2009, 2010a).

Furthermore, another member of this class, SN 2008ge, was hosted in an S0 galaxy with no signs of star formation or massive stars, including at the SN position in pre-explosion *Hubble Space Telescope* (*HST*) images (Foley et al. 2010c). SN 2008ge most likely had a WD progenitor. SN 2008ha had an inferred ejecta mass of $\sim 0.3\ M_\odot$, which is less than the total mass of any WD expected to explode as an SN. If SN 2008ha had a WD progenitor, then its progenitor star was not completely disrupted during the explosion (Foley 2008; Foley et al. 2009, 2010a).

Although there have been a number of papers on individual members of this class (Li et al. 2003; Branch et al. 2004; Chornock et al. 2006; Jha et al. 2006; Phillips et al. 2007; Sahu et al. 2008; Foley et al. 2009, 2010a, 2010c; Valenti et al. 2009; Maund et al. 2010; McClelland et al. 2010; Narayan et al. 2011; Kromer et al. 2012), a holistic view of the entire class has not yet been published. Here, we present new data for several SNe and examine the properties of all known members of the class, totaling 25 SNe, with the intention of further understanding the relations between observational properties of the class, their progenitor systems, and their explosions.

The manuscript is structured in the following way. Section 2 outlines the criteria for membership in the class and details the members of the class. We present previously published and new observations of the SNe in Section 3. We describe the photometric and spectroscopic properties of the class in Sections 4 and 5, respectively. In Section 6, we provide estimates of the relative rate of SNe Iax to normal SNe Ia and the Fe production from SNe Iax. We summarize the observations and constrain possible progenitor systems in Section 7, and we conclude in Section 8. UT dates are used throughout the paper.

## 2. MEMBERS OF THE CLASS

SNe have historically been classified spectroscopically (Minkowski 1941), with the presence or absence of particular spectral features being the fundamental distinction between various classes. Occasionally, photometric properties are used to subclassify various classes (e.g., SNe IIL and IIP). Recently, the underlying diversity of SNe combined with the recent surge in discoveries has blurred clear lines in SN classification.

Observational classification has several advantages over "theoretical" classification. Observational classification is purely empirical, which has previously linked physically unrelated objects. For instance, SNe I used to be a single class. Even with these potential mistakes, this kind of classification has been exceedingly useful for determining the physical underpinnings of stellar explosions. On the other hand, ascribing particular theoretical models to perform classification indicates a "correct" model and can hinder further advancements. Here, we attempt to provide an observational classification scheme for the SN Iax class.

The primary motivation of this classification scheme is to include all SNe physically similar to SN 2002cx without including those with significantly different progenitors or explosion mechanisms; however, further refinements may be necessary in the future. We exclusively use observational properties of the SNe to provide the classification.

As noted above, SNe Iax are somewhat spectroscopically similar to the high-luminosity SN Ia 1991T. Figure 1 shows the near-maximum-brightness spectra of three SNe Iax. These SNe have ejecta velocities that range from $|v| = 2200$ to 6900 km s$^{-1}$. By artificially smoothing the spectra (Blondin & Tonry 2007) to broaden the spectral features and also blueshifting the spectra, one can produce spectra that are similar to what one would expect if the SN simply had a higher ejecta velocity. Doing this exercise, one can see the continuum from SN 2009J (with $|v| = 2200$ km s$^{-1}$) through SN 2005cc (with $|v| = 5200$ km s$^{-1}$) to SN 2008A (with $|v| = 6900$ km s$^{-1}$). All SNe Iax seem to have similar composition with varying ejecta velocity. SNe Iax also appear to be similar to high-luminosity SNe Ia, such as SN 1991T and SN 1999aa (Li et al. 2001b; Garavini et al. 2004), near maximum brightness after accounting for ejecta velocity. Since the individual narrow lines in SNe Iax are the same lines seen as blends in SNe Ia, identifying features in SNe Iax helps with interpreting SN Ia spectra.

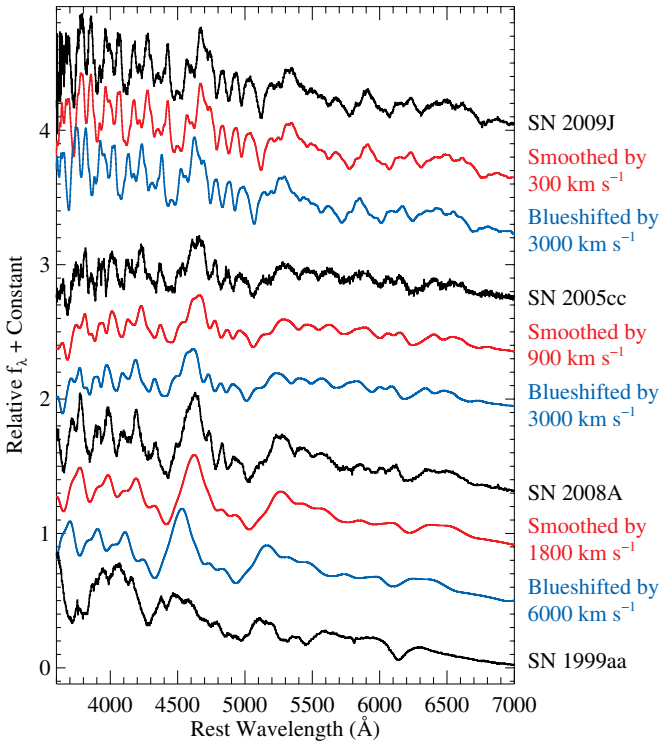


**Figure 1.** Spectra of SNe Iax, from lowest to highest ejecta velocity (SNe 2009J, 2005cc, and 2008A, respectively), in comparison with the high-luminosity SN Ia 1999aa (Li et al. 2001b; Garavini et al. 2004). The black spectra are unaltered. The red spectra are smoothed using a Gaussian filter of 300, 900, and 1800 km s$^{-1}$ for SNe 2009J, 2005cc, and 2008A, respectively. The blue spectra are the smoothed spectra after being blueshifted by 3000, 3000, and 6000 km s$^{-1}$, respectively. The smoothed, blueshifted SN 2009J spectrum is visually similar to the unaltered SN 2005cc spectrum; the smoothed, blueshifted SN 2005cc spectrum is visually similar to the unaltered SN 2008A spectrum; and the smoothed, blueshifted SN 2008A spectrum is visually similar to the unaltered SN 1999aa spectrum.

(A color version of this figure is available in the online journal.)

To be a member of the SN Iax class, we require (1) no evidence of hydrogen in any spectrum, (2) a maximum-brightness photospheric velocity lower than that of any normal SN Ia at maximum brightness ($|v| \lesssim 8000$ km s$^{-1}$), and (3) if near-maximum light curves are available, an absolute magnitude that is low for a normal SN Ia given its light-curve shape (i.e., falling below the WLR for SNe Ia). By the first criterion, we exclude all SNe II and any SN that obviously has a hydrogen envelope. The second criterion will exclude all "normal" SNe Ia, Ib, and Ic, including high-luminosity and low-luminosity SNe Ia similar to SN 1991T (Filippenko et al. 1992b; Phillips et al. 1992) and SN 1991bg (Filippenko et al. 1992a; Leibundgut et al. 1993), respectively, as well as the unique SN 2000cx (Li et al. 2001a), SNe similar to SN 2006bt (Foley et al. 2010b), SN 2010X (Kasliwal et al. 2010), and ultraluminous SNe I (e.g., Pastorello et al. 2010; Quimby et al. 2011; Chomiuk et al. 2011). No known core-collapse SN passes these first two criteria. The third criterion excludes all "super-Chandrasekhar" SNe Ia (e.g., Howell et al. 2006), which can have low ejecta velocities, but have high peak luminosities.

A final criterion is that the spectra need to be similar to those of SN 2002cx at comparable epochs. This last criterion is somewhat subjective, yet necessary. It is also a primary criterion, as the first two criteria listed above naturally result from spectral similarity. We note that this criterion is no more subjective than the one used to distinguish between SNe Ia and Ic. However, exclusively using the previously listed criteria for classification would include specific SNe that do not appear to be physically related to SN 2002cx. For instance, SN 2005E (Perets et al. 2010) lacks hydrogen, has a low ejecta velocity, and a low luminosity for its light-curve shape, but is clearly spectroscopically different from SN 2002cx at all epochs. SNe 2005E and 2008ha have somewhat similar spectra at ∼2 months after maximum brightness. Both have strong [Ca II] and Ca II emission, but there are several significant differences, including SN 2008ha lacking [O I] (Foley et al. 2009). Significant differences in the host-galaxy morphologies for SNe similar to SNe 2002cx and 2005E further suggest that these SNe have significantly different progenitor systems (Foley et al. 2009; Perets et al. 2010). SNe 2002es (Ganeshalingam et al. 2012) and PTF 09dav (Sullivan et al. 2011, which fails our first criterion) have low luminosity and low velocities, but also have significantly cooler spectra (lacking Fe III and having strong Ti II features) than SN 2002cx near maximum brightness. Although SN 2002es and PTF 09dav may be physically related to the SN 2002cx-like class in the same way that SN 1991bg is similar to the hotter, more common "Branch-normal SNe Ia" (Branch et al. 1993), we do not currently link these SNe to SNe Iax. The progenitor environments of the SN 2002es and PTF 09dav are also suggestive of older progenitor systems: SN 2002es was hosted in an S0 galaxy, a fairly unusual host for an SN Iax (Foley et al. 2009), and PTF 09dav was found ∼40 kpc from its host, which may indicate a particularly old progenitor system, unlike what is inferred for the majority of SNe Iax. We also exclude SN 2002bj (Poznanski et al. 2010), which is somewhat spectroscopically similar to SN 2002cx, but also different in several ways. Its light curve was extremely fast ($\Delta m_{15} > 4$ mag), yet it was still fairly luminous at peak ($M \approx -18$ mag). We consider there to be too many significant differences to include SN 2002bj in the class. A list of our criteria and how various SN classes and particular objects pass or fail the criteria is presented in Table 1.

When applying the criteria to our sample, we note that three of the four criteria can be determined from a single spectrum near maximum light. We also note that there are no SNe that are spectroscopically similar to SN 2002cx and also have luminosities equal to or larger than SNe Ia with the same light-curve shape. Therefore, a single near-maximum-light spectrum appears to be sufficient for classification. However, because of the spectral similarities with other SNe Ia (except for the lower ejecta velocities; see Figure 1), SNe Iax are easily mistaken as normal SNe Ia in initial classifications. In particular, spectral classification software such as SNID (Blondin & Tonry 2007) can easily misclassify an SN Iax as an SN 1991T-like SN Ia if one does not know the redshift of the SN or does not restrict the redshift to be the host-galaxy redshift. Misclassification was even more common before the recognition of SN 2002cx as being distinct from SNe Ia and before a substantial set of examples was assembled. We therefore do not believe that our sample is complete, and it could be significantly incomplete (especially for SNe discovered before 2002). However, the CfA and Berkeley Supernova Ia Program (BSNIP) spectral samples have been searched for misclassified SNe Iax (Blondin et al. 2012; Silverman et al. 2012), with BSNIP identifying one new SN Iax. When determining membership in the class, we first examine our own and published data to match the criteria described above. For some objects, we use data from IAU Circulars and The Astronomer's Telegrams. There is no definitively identified SN Iax for which we do not have

**Table 1**
Classification Criteria for SNe Iax

| SN Class | Has Hydrogen? | $\|v\| \lesssim 8000$ km s$^{-1}$? | Low $L$ for LC Shape | Spec. like SN 2002cx |
|---|---|---|---|---|
| **SN Iax** | **N** | **Y** | **Y** | **Y** |
| SN II | Y | Some | N/A | N |
| SN Ib/c | N | N | Y | N |
| SLSN I | N | Y | N | N |
| Normal SN Ia | N | N | N | N |
| Super-Chandra | N | Y | N | N |
| SN 1991T | N | N | N | Somewhat |
| SN 1991bg | N | N | N | N |
| SN 2000cx | N | N | Y | N |
| SN 2002bj | N | Y | N | Somewhat |
| SN 2002es | N | Y | Y | Somewhat |
| SN 2002ic | Y | N | N | N |
| SN 2005E | N | Y | Y | N |
| SN 2006bt | N | N | Y | N |
| SN 2010X | N | N | Y | N |
| PTF 09dav | Y | Y | Y | Somewhat |

access to previously published data or our own data published here.

There are currently 25 known SNe Iax.[14] Fifteen of these SNe were considered members of the class by Foley et al. (2009). Since that publication, six additional members have been discovered and four previously known SNe have been identified as members. The sample size is considerable; the original Type I/II SN classification and the definition of the SN IIP/IIL, SN IIn, SN IIb, and broad-lined SN Ic classes were all performed with significantly fewer members of each class. A list of the members and some of their basic properties are in Table 2.

Below, we present details for the SNe. For additional information, see Foley et al. (2009) and references therein, and the references listed for each SN below.

### 2.1. SN 1991bj

SN 1991bj is the oldest known member of the class, although it has only recently been identified as a member (Foley et al. 2009). It was originally classified as an SN Ia by two separate teams (Pollas et al. 1992). Gomez et al. (1996) presented a spectrum of SN 1991bj and noted its low ejecta velocity. Stanishev et al. (2007) first identified SN 1991bj as a possible SN Iax. Foley et al. (2009) used a Lick spectrum obtained by A. V. Filippenko to classify SN 1991bj as an SN Iax.

### 2.2. SN 1999ax

SN 1999ax was discovered by the Wise Observatory Optical Transient Search (WOOTS; Gal-Yam et al. 2008) in the field of A1852, which has a redshift $z = 0.181$ (Gal-Yam & Maoz 1999). Spectra of the SN suggested that SN 1999ax was an SN Ia at $z \approx 0.05$ (Gal-Yam et al. 2000). A spectrum was also presented by Gal-Yam et al. (2008), where they used template matching to find $z \approx 0.05$.[15]

However, a Sloan Digital Sky Survey (SDSS) spectrum revealed that its host galaxy, SDSS J140358.27+155101.2, is at $z = 0.023$ (Abazajian et al. 2009). We obtained the spectrum of SN 1999ax from 1999 April 6,[16] but its flux calibration does not appear to be correct. To make a comparison to other SNe, we divided the flux by a fifth-order polynomial and compared the resulting spectrum to other SN spectra that were similarly modified. Using the SDSS redshift and correcting the flux, it is clear that SN 1999ax is similar to SN 2002cx (see Figure 2).

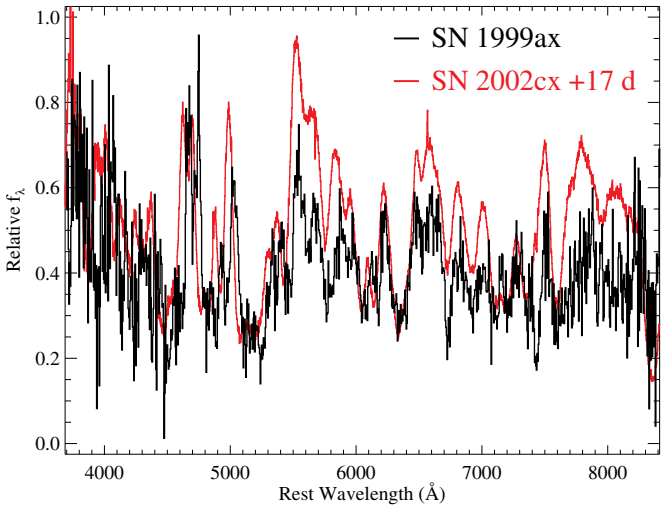


**Figure 2.** Spectra of SN 1999ax (black) and SN 2002cx (red). Both spectra have been divided by a fifth-order polynomial to remove the poor flux calibration of the SN 1999ax spectrum and to make an appropriate comparison. The rest-frame phase relative to $V$ maximum is marked for SN 2002cx.

(A color version of this figure is available in the online journal.)

This is the first time that SN 1999ax has been considered a member of the SN Iax class.

### 2.3. SN 2002bp

SN 2002bp was discovered by the Puckett Observatory Supernova Search (POSS; Puckett & Langoussis 2002), but remained unclassified for several years. Finally, while analyzing the large BSNIP sample of SN Ia spectra, Silverman et al. (2012) determined that SN 2002bp was similar to SN 2008ha, another member of this class.

[14] In the final stages of the preparation of this manuscript, LSQ12fhs, SN 2006ct, and PS1-12bwh were identified as potential SNe Iax. At the time of publication, we had not verified the classifications (Copin et al. 2012; Quimby et al. 2012; Wright et al. 2012).

[15] Gal-Yam et al. (2008) also note that their spectrum of SN 1999ax is "somewhat peculiar," but do not expand further since it was not the focus of their study.

[16] Spectra are available at http://www.physto.se/~snova/private/near-z/spectroscopy/reduced_data/.

**Table 2**
Properties of SNe Iax

| SN Name | R.A. (J2000) | Dec. (J2000) | Refs. | $t_{max}(V)$ (JD − 2,450,000) | $M_{V,peak}$ (mag) | $\Delta m_{15}(V)$ (mag) | $v_peak$ ( km s$^{-1}$) | He? |
|---|---|---|---|---|---|---|---|---|
| 1991bj | 03:41:30.47 | −04:39:49.5 | 1,2,3 | ... | $\lesssim$−15.4 | ... | ... | N |
| 1999ax | 14:03:57.92 | +15:51:09.2 | 4,5 | ... | $\lesssim\lesssim$−16.4 | ... | ... | N |
| 2002bp | 11:19:18.20 | +20:48:23.1 | 6 | ... | $\lesssim\lesssim$−16.1 | ... | ... | N |
| 2002cx | 13:13:49.72 | +06:57:31.9 | 7,8,9 | 2418.31 | −17.63 | 0.84 | −5600 | N |
| 2003gq | 22:53:20.68 | +32:07:57.6 | 9,10 | 2852.56 | −17.29 | 0.98 | −5200 | N |
| 2004cs | 17:50:14.38 | +14:16:59.5 | 4,11 | ∼3185 | ∼−16.2 | ∼1.4 | ... | Y |
| 2004gw | 05:08:48.41 | +62:26:20.7 | 1,12,13 | ... | $\lesssim\lesssim$−16.4 | ... | ... | N |
| 2005P | 14:06:34.01 | −05:27:42.6 | 4,9,14 | ... | $\lesssim\lesssim$−15.3 | ... | ... | N |
| 2005cc | 13:57:04.85 | +41:50:41.8 | 15,16 | 3522.10 | −16.48 | 0.97 | −5000 | N |
| 2005hk | 00:27:50.89 | −01:11:53.3 | 17,18,19 | 3689.81 | −18.37 | 0.92 | −4500 | N |
| 2006hn | 11:07:18.67 | +76:41:49.8 | 1,20,21 | >3895.0 | <−17.7 | ... | ... | N |
| 2007J | 02:18:51.70 | +33:43:43.3 | 1,4,22,23 | 4075.7–4114.3 | $\lesssim$−15.4 | ... | ... | Y |
| 2007ie | 22:17:36.69 | +00:36:48.0 | 25,26 | <4348.5 | ∼−18.2 | ... | ... | N |
| 2007qd | 02:09:33.56 | −01:00:02.2 | 24 | 4353.9–4404.4 | ... | ... | ... | N |
| 2008A | 01:38:17.38 | +35:22:13.7 | 16,27,28,29 | 4483.61 | −18.46 | 0.82 | −6400 | N |
| 2008ae | 09:56:03.20 | +10:29:58.8 | 4,27,30,31 | 4513.52 | −17.67 | 0.94 | −6100 | N |
| 2008ge | 04:08:24.68 | −47:53:47.4 | 14 | 4725.77 | −17.60 | 0.34 | ... | N |
| 2008ha | 23:34:52.69 | +18:13:35.4 | 1,32,33 | 4785.24 | −14.19 | 1.22 | −3200 | N |
| 2009J | 05:55:21.13 | −76:55:20.8 | 4,34 | >4836.6 | $\lesssim\lesssim$−16.6 | ... | −2200 | N |
| 2009ku | 03:29:53.23 | −28:05:12.2 | 35,36 | ... | −18.94 | 0.38 | ... | N |
| 2010ae | 07:15:54.65 | −57:20:36.9 | 4,37 | >5244.6 | $\lesssim\lesssim$−14.9 | ... | ... | N |
| 2010el | 04:19:58.83 | −54:56:38.5 | 38 | >5350.6 | $\lesssim\lesssim$−14.8 | ... | ... | N |
| 2011ay | 07:02:34.06 | +50:35:25.0 | 4,39 | 5651.81 | −18.40 | 0.75 | −5600 | N |
| 2011ce | 18:55:35.84 | −53:43:29.1 | 4,40 | 5658–5668 | −17.8 – −18.9 | 0.4 – 1.3 | ... | N |
| 2012Z | 03:22:05.35 | −15:23:15.6 | 4,41 | >5955.7 | $\lesssim$−16.8 | ... | ... | N |

**References.** (1) Foley et al. 2009; (2) Gomez et al. 1996; (3) Stanishev et al. 2007; (4) This Paper; (5) Gal-Yam et al. 2008; (6) Silverman et al. 2012; (7) Li et al. 2003; (8) Branch et al. 2004; (9) Jha et al. 2006; (10) Filippenko & Chornock 2003; (11) Rajala et al. 2005; (12) Foley & Filippenko 2005; (13) Filippenko & Foley 2005; (14) Foley et al. 2010c; (15) Antilogus et al. 2005; (16) Ganeshalingam et al. 2010; (17) Chornock et al. 2006; (18) Phillips et al. 2007; (19) Sahu et al. 2008; (20) Foley et al. 2006; (21) Hicken et al. 2009; (22) Filippenko et al. 2007a; (23) Filippenko et al. 2007b; (24) McClelland et al. 2010; (25) Bassett et al. 2007b; (26) Östman et al. 2011; (27) Blondin & Berlind 2008; (28) Hicken et al. 2012; (29) C. McCully et al., in preparation; (30) Blondin & Calkins 2008; (31) Milne et al. 2010 (32) Foley et al. 2010a; (33) Valenti et al. 2009; (34) Stritzinger 2009; (35) Rest et al. 2009; (36) Narayan et al. 2011; (37) Stritzinger et al. 2010b; (38) Bessell et al. 2010; (39) Silverman et al. 2011a; (40) Anderson & Morrell 2011; (41) Cenko et al. 2012.

### 2.4. SN 2002cx

SN 2002cx was the first SN in this class recognized as being peculiar and is its namesake. Wood-Vasey et al. (2002) discovered SN 2002cx on 2002 May 12. Basic observational information derived from near-maximum data were originally presented by Li et al. (2003). The photometric data were re-evaluated by Phillips et al. (2007). Late-time spectra were presented by Jha et al. (2006). Branch et al. (2004) performed a detailed spectral analysis of its maximum-light spectra.

### 2.5. SN 2003gq

SN 2003gq was independently discovered (Graham et al. 2003; Puckett et al. 2003) by the Lick Observatory Supernova Search (LOSS; Li et al. 2000; Filippenko et al. 2001) and POSS. It was originally classified as an SN Ia by Filippenko et al. (2003) and was later revised as an SN Iax (Filippenko & Chornock 2003). As part of the LOSS photometric follow-up effort, filtered photometry of SN 2003gq was obtained and presented by Ganeshalingam et al. (2010). Blondin et al. (2012) presented a spectrum of SN 2003gq.

### 2.6. SN 2004cs

Li et al. (2004) discovered SN 2004cs as part of LOSS. Rajala et al. (2005) presented its spectrum and classified it as an SN IIb, identifying both H$\alpha$ and strong He I features. We obtained this spectrum (via D. Leonard), and show a comparison of

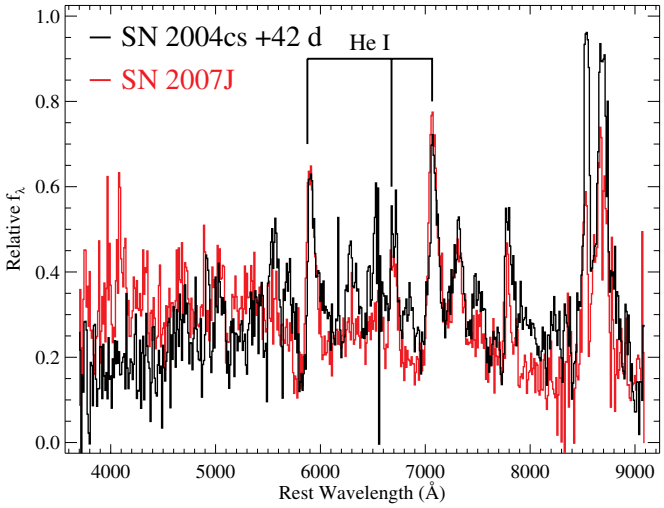


**Figure 3.** Spectra of SN 2004cs (black) and SN 2007J (red). The approximate rest-frame phase relative to $V$ maximum is marked for SN 2004cs.
(A color version of this figure is available in the online journal.)

SNe 2004cs and 2007J in Figure 3. Both SNe are very similar, and SN 2004cs clearly has He I features. However, we do not identify H$\alpha$ in the spectrum; there are clear residuals from galaxy subtraction at the position of H$\alpha$, but the peak of the feature is also blueward of H$\alpha$. SN 2007J was identified as a

member of the SN Iax class, but showed He I lines (Foley et al. 2009). SN 2004cs demonstrates that there is more than one member of this class that exhibits He in its spectrum.

This is the first time that SN 2004cs has been considered an SN Iax. In Section 3.1, we present a previously unpublished unfiltered light curve obtained with the robotic 0.76 m Katzman Automatic Imaging Telescope (KAIT; Filippenko et al. 2001) at Lick Observatory.

### 2.7. SN 2004gw

SN 2004gw was discovered by POSS on 2004 December 29 (Puckett & Ireland 2004). Gal-Yam (2005) originally classified it as an SN I with some indications that it was of Type Ic. Foley & Filippenko (2005) suggested that it was an SN Ia which "exhibits a number of spectral peculiarities." Filippenko & Foley (2005) later confirmed that it was of Type Ia. Finally, with the aid of a larger comparison sample, Foley et al. (2009) showed that SN 2004gw was an SN Iax.

### 2.8. SN 2005P

SN 2005P was discovered by LOSS on 2005 January 21 (Burket & Li 2005b). Visual inspection of unpublished data taken on 2005 January 22 by Schmidt & Salvo (2005, private communication) indicates that it is an SN Iax. The SN remained unclassified in the literature for over a year. Based on a late-time spectrum, Jha et al. (2006) classified it as an SN Iax. Foley et al. (2010c) later suggested that SN 2005P was spectroscopically most similar to SN 2008ge, having a late-time spectrum with relatively broad lines and relatively strong forbidden Fe lines. We present a previously unpublished KAIT unfiltered light curve in Section 3.1.

### 2.9. SN 2005cc

SN 2005cc was discovered by POSS on 2005 May 19 (Puckett et al. 2005). Several spectra indicated that it was a young SN similar to SN 2002cx (Antilogus et al. 2005). As a part of the LOSS photometric follow-up effort, filtered photometry of SN 2005cc was obtained and presented by Ganeshalingam et al. (2010). Spectra of SN 2005cc were presented by Blondin et al. (2012).

### 2.10. SN 2005hk

SN 2005hk, which was independently discovered by both LOSS (Burket & Li 2005a) and SDSS-II (Barentine et al. 2005), is the best-observed SN Iax. Phillips et al. (2007) and Sahu et al. (2008) presented extensive data near maximum brightness. Kromer et al. (2012) presented NIR spectra and late-time photometry of SN 2005hk, while Sahu et al. (2008) and Valenti et al. (2009) published late-time spectra. Chornock et al. (2006) and Maund et al. (2010) showed spectropolarimetric observations indicating that SN 2005hk had low polarization near maximum brightness. Late-time spectroscopy and *HST* photometry will be presented by C. McCully et al. (in preparation).

### 2.11. SN 2006hn

POSS discovered SN 2006hn on 2006 September 28 (Sehgal et al. 2006). Foley et al. (2006) classified SN 2006hn as an SN Ia, and Foley et al. (2009) noted that it was an SN Iax. Photometry of SN 2006hn was published as part of the CfA3 data release (Hicken et al. 2009).

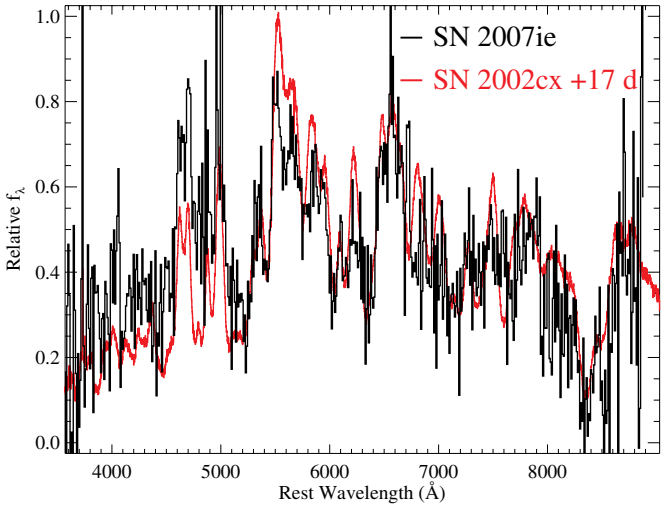


**Figure 4.** Spectra of SN 2007ie (black; galaxy subtracted) and SN 2002cx (red). The rest-frame phase relative to *V* maximum is marked for SN 2002cx.

(A color version of this figure is available in the online journal.)

### 2.12. SN 2007J

SN 2007J, which was independently discovered by both LOSS and POSS (Lee et al. 2007), was the first known member of the SN Iax class to display He I lines. Initially, these lines were weak, and SN 2007J appeared to be very similar to SN 2002cx (Filippenko et al. 2007a); however, the He I lines became stronger with time, causing Filippenko et al. (2007b) to reclassify SN 2007J as a peculiar SN Ib. Foley et al. (2009) re-examined the spectra, showing that besides the He I lines, SN 2007J is indeed very similar to SN 2002cx. We therefore consider SN 2007J to be a peculiar SN Iax. We present previously unpublished KAIT filtered and unfiltered light curves in Section 3.1.

### 2.13. SN 2007ie

SN 2007ie was discovered by SDSS-II (Bassett et al. 2007b), who also classified it as a probable SN Ia. Östman et al. (2011) presented a spectrum of SN 2007ie and indicated that it was a probable SN Iax. They noted the low velocity and spectral similarities to SNe 2002cx and 2005hk, but allowed the possibility that it was a normal SN Ia. However, restricting the redshift of the comparison spectra to that of SN 2007ie, only SNe Iax provide reasonable matches. Additionally, the peak magnitude is $M \approx -18.2$ mag, similar to that of SN 2002cx, although the peak of the light curve was not covered in their photometry. Figure 4 shows the galaxy-subtracted spectrum of SN 2007ie compared to SN 2002cx. We consider SN 2007ie to be a clear member of the SN Iax class.

### 2.14. SN 2007qd

SN 2007qd was discovered by SDSS-II (Bassett et al. 2007a). It is a relatively faint SN Iax with ejecta velocity between those of SNe 2002cx and 2008ha (McClelland et al. 2010). McClelland et al. (2010) used observations of SNe 2002cx, 2005hk, 2007qd, and 2008ha to argue that there was a relationship between ejecta velocity and peak absolute magnitude for SNe Iax. Narayan et al. (2011) showed that SN 2009ku was a prominent outlier to this trend.

### 2.15. SN 2008A

SN 2008A was discovered on 2008 January 2 by Nakano et al. (2008). It was classified as an SN Iax by Blondin & Berlind (2008). As a part of the LOSS photometric follow-up effort, filtered photometry of SN 2008A was obtained and presented by Ganeshalingam et al. (2010). Photometry of SN 2008A was also published as part of the CfA4 data release (Hicken et al. 2012). The SN was observed photometrically by *Swift*; Milne et al. (2010) found that SNe Iax have very blue UV colors relative to normal SNe Ia. Spectroscopy and late-time *HST* photometry will be presented by C. McCully et al. (in preparation). Blondin et al. (2012) presented several spectra of SN 2008A.

### 2.16. SN 2008ae

POSS discovered SN 2008ae on 2008 February 9 (Sostero et al. 2008). Blondin & Calkins (2008) classified it as an SN Iax, and they further note that SN 2008ae is relatively luminous ($M < -17.7$ mag) a few days before maximum brightness. Optical and UV photometry of SN 2008ae was also published as part of the CfA4 data release (Hicken et al. 2012) and the *Swift* photometry compilation (Milne et al. 2010), respectively. Blondin et al. (2012) presented several spectra of SN 2008ae. We present previously unpublished KAIT and Carnegie Supernova Project (CSP) light curves in Section 3.1.

### 2.17. SN 2008ge

SN 2008ge was very nearby and bright. It was discovered by CHASE (Pignata et al. 2008) well past maximum brightness, but CHASE had several pre-discovery images from which a light curve could be generated. Its host galaxy, NGC 1527, is an S0 galaxy with no signs of star formation to deep limits ($<7.2 \times 10^{-3}\ M_{\odot}\ \mathrm{yr}^{-1}$; Foley et al. 2010c). It was also imaged by *HST* before SN 2008ge occurred, and analysis showed that there were no massive stars near the SN site or any indication of star formation in the host galaxy (Foley et al. 2010c).

SN 2008ge had a relatively broad light curve and (unlike SNe 2002cx and 2005hk) strong [Fe II] emission lines in its late-time spectra (Foley et al. 2010c). The lack of massive stars near the SN site, the strict limit on the star-formation rate, and the presumably large generated $^{56}$Ni mass all suggest a WD progenitor (Foley et al. 2010c).

### 2.18. SN 2008ha

SN 2008ha is an extreme SN Iax, being less luminous than any other member and having lower ejecta velocity than most members of the class (Foley et al. 2009, 2010a; Valenti et al. 2009). It was discovered by POSS (Puckett et al. 2008).

Several studies have been devoted to SN 2008ha (Foley et al. 2009, 2010a; Valenti et al. 2009), and details of the SN are presented in those works. Notably, the total inferred ejecta mass is significantly below the Chandrasekhar mass. Although SN 2008ha may have had a massive-star progenitor (Foley et al. 2009; Valenti et al. 2009), carbon/oxygen burning products in its maximum-light spectrum, and the energy/ejecta mass balancing necessary to create a low-velocity, low-luminosity SN like SN 2008ha make that scenario unlikely (Foley et al. 2009, 2010a).

### 2.19. SN 2009J

CHASE discovered SN 2009J on 2009 January 13 (Pignata et al. 2009). Follow-up spectroscopy revealed that it was a SN Iax (Stritzinger 2009). SN 2009J is a particularly low-velocity SN, similar to, but even lower velocity than SN 2008ha (Figure 5). We present previously unpublished CSP and CHASE light curves in Section 3.1 and previously unpublished spectra in Section 3.2.

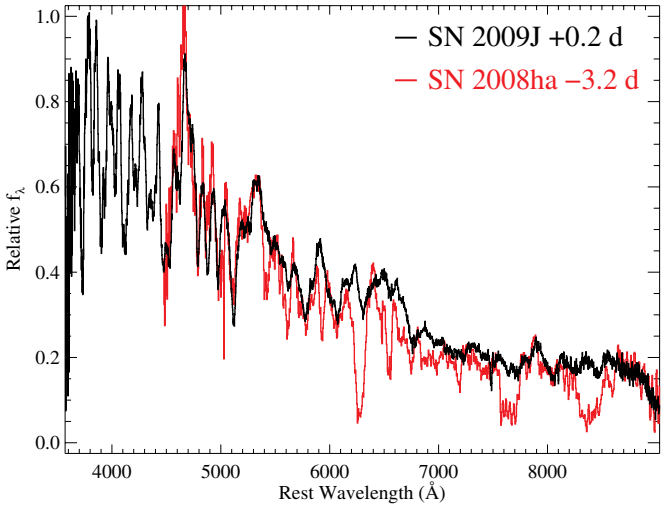


**Figure 5.** Spectra of SN 2009J (black) and SN 2008ha (red). The rest-frame phase relative to *V* maximum is marked for both SNe.

(A color version of this figure is available in the online journal.)

### 2.20. SN 2009ku

SN 2009ku was discovered by Pan-STARRS1 (PS1; Rest et al. 2009), and Narayan et al. (2011) presented detailed observations. SN 2009ku is a relatively luminous SN Iax ($M_{V,\mathrm{peak}} \approx -18.4$ mag), but had ejecta velocity comparable to that of the extremely low-luminosity SN 2008ha. This showed that, contrary to what was presented by McClelland et al. (2010), velocity and luminosity are not strongly correlated for all SNe Iax (Narayan et al. 2011).

### 2.21. SN 2010ae

SN 2010ae was discovered on 2010 February 23 in ESO 162-G017 (Pignata et al. 2010). Stritzinger et al. (2010a) originally classified it as a peculiar SN Ia similar to the possible "super-Chandrasekhar" SN 2006gz (Hicken et al. 2007). Using additional data, Stritzinger et al. (2010b) determined that SN 2010ae was most similar to SN 2008ha. In Figure 6, we present a spectrum at an epoch similar to those from Stritzinger et al. (2010b) that shows this similarity to SN 2008ha (although with a slightly different continuum shape). A full analysis of SN 2010ae will be presented by M. Stritzinger et al. (in preparation).

### 2.22. SN 2010el

SN 2010el was discovered on 2010 June 19 in NGC 1566 (Monard 2010). Bessell et al. (2010) determined that SN 2010el was spectroscopically similar to SN 2008ha. A full analysis of SN 2010el will be presented by S. Valenti et al. (in preparation).

### 2.23. SN 2011ay

SN 2011ay was discovered on 2011 March 18 in NGC 2314 as part of LOSS (Blanchard et al. 2011). Pogge et al. (2011) classified SN 2011ay as an SN Ia similar to the high-luminosity SN 1999aa (Li et al. 2001b; Garavini et al. 2004). However, Silverman et al. (2011a) later classified SN 2011ay as an

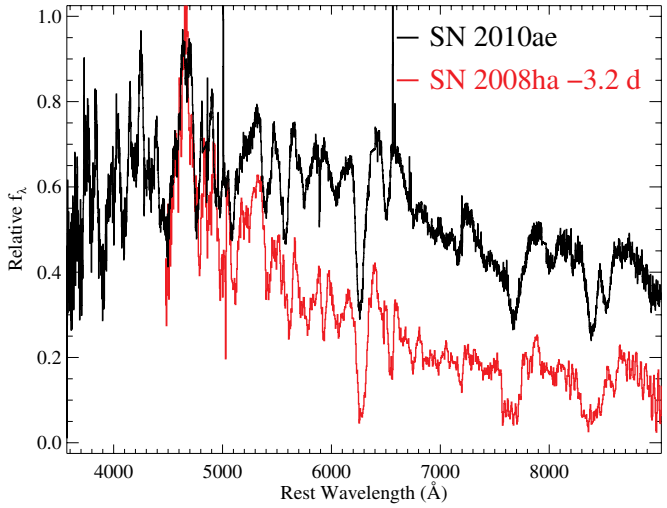


**Figure 6.** Spectra of SN 2010ae (black) and SN 2008ha (red). Although the continua have different shapes, the spectral features are similar. The rest-frame phase relative to $V$ maximum is marked for SN 2008ha.

(A color version of this figure is available in the online journal.)

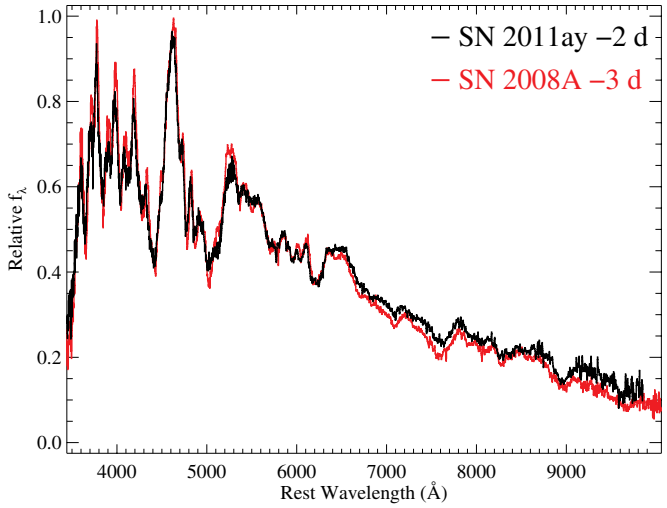


**Figure 7.** Spectra of SN 2011ay (black) and SN 2008A (red). The rest-frame phase relative to $V$ maximum is marked for both SNe.

(A color version of this figure is available in the online journal.)

SN Iax. Spectra of SNe 2011ay and 2008A are shown in Figure 7. SN 2011ay is clearly an SN Iax. We present previously unpublished CfA light curves in Section 3.1 and previously unpublished spectra in Section 3.2.

### 2.24. SN 2011ce

SN 2011ce was discovered on 2011 March 26 in NGC 6708 (Maza et al. 2011), although it was not announced until about a month later. There was a nondetection on 2011 March 4. Soon after the announcement, on 2011 April 24, Anderson & Morrell (2011) classified SN 2011ce as an SN Iax with a phase of about 20 days after maximum brightness.

We present a previously unpublished, unfiltered CHASE light curve in Section 3.1. Using the light curve of SN 2005hk, and allowing for a range of light-curve stretches, we find that SN 2011ce likely peaked between 2011 April 7 and 17 with a peak unfiltered magnitude of $-17.6$ to $-18.7$ (corresponding

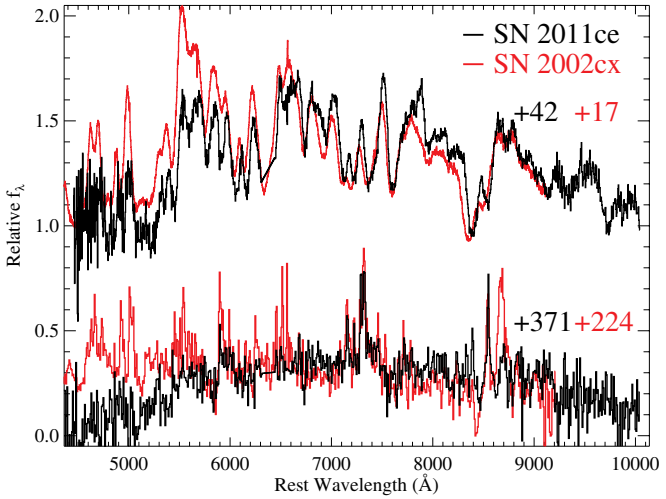


**Figure 8.** Spectra of SN 2011ce (black) and SN 2002cx (red). The approximate rest-frame phase relative to $V$ maximum is marked for all spectra.

(A color version of this figure is available in the online journal.)

roughly to $-17.8 \geqslant M_V \geqslant -18.3$ mag). We obtained optical spectra on 2011 April 24 and on 2012 April 20, more than a year after discovery. The spectra are 47/409 and 37/360 rest-frame days after the last nondetection and the first detection, respectively, and ∼42 and 371 rest-frame days after maximum brightness, respectively.

A comparison of our SN 2011ce spectra and those of SN 2002cx is shown in Figure 8. SN 2011ce is clearly a SN Iax, at early times being similar to SN 2002cx, and at late times displaying low-velocity P-Cygni profiles of Fe as well as strong [Ca II] and Ca II emission lines.

### 2.25. SN 2012Z

SN 2012Z was discovered on 2012 January 29 in NGC 1309 by LOSS (Cenko et al. 2012). Cenko et al. (2012) also report spectroscopic observations indicating that SN 2012Z is an SN Iax. A detailed study of this SN and its progenitor will be presented by W. Fong et al. (in preparation). A comparison of the spectra of SNe 2002cx and 2012Z is shown in Figure 9. We present previously unpublished CfA light curves in Section 3.1.

### 2.26. Possible Subclasses

Based on the criteria outlined above, we have selected the members of the SN Iax class in the previous subsections. As mentioned above, the inclusion and exclusion of particular SNe is somewhat subjective. Here, we focus on possible subclasses of SNe Iax that could be physically different from the other members. The two obvious groups (which may be considered subclasses of SNe Iax) are the SNe similar to SNe 2007J and 2008ha, respectively.

Unlike other members of the class, SNe 2004cs and 2007J both have strong He I lines in their spectra. It is still unclear if this difference is the result of different ejecta (SNe 2004cs and 2007J have significantly more helium in their ejecta than other members), different physical conditions (such as ionization at a given time), or an observational effect (only particular viewing angles show He I, or the lines are only present at particular phases). Additional observations with significantly more data should help disentangle these possibilities. Until there is a clear physical difference, we include these objects in the class, with

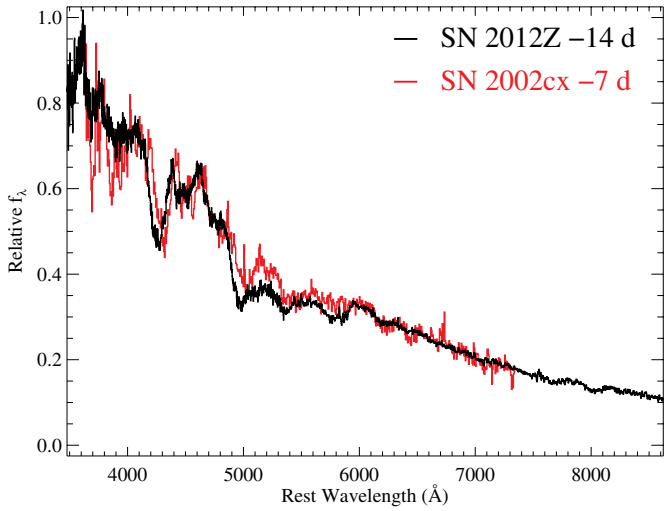


**Figure 9.** Spectra of SN 2012Z (black) and SN 2002cx (red). The rest-frame phase relative to *V* maximum is marked for both SNe.

(A color version of this figure is available in the online journal.)

the He I lines being an interesting constraint on the progenitor systems and explosion.

Several members of the class (SNe 2002bp, 2009ku, 2010ae, and 2010el) have extremely low velocity ($|v| \approx 3{,}000$ km s$^{-1}$), similar to SN 2008ha. Although this is a possible indication of a distinct subclass, other observations conflict with this possibility. Specifically, there is a range of ejecta velocities for the class (see Section 5), and there appears to be a continuous sequence of velocities (McClelland et al. 2010). Additionally, SN 2009ku had very low velocities but a luminosity similar to that of SN 2002cx (Narayan et al. 2011), indicating that the SNe with very low velocity are not distinct in all properties. We consider these objects to be extreme members of the class rather than a separate group.

## 3. OBSERVATIONS AND DATA REDUCTION

### *3.1. Photometry*

Below, we present new and previously published photometry of several SNe Iax. SNe 2003gq, 2005cc, and 2008A have previously published filtered photometry from KAIT (Ganeshalingam et al. 2010). The KAIT photometry is supplemented by previously published photometry of SNe 2006hn, 2008A, and 2008ae from the CfA3 (Hicken et al. 2009) and CfA4 (Hicken et al. 2012) samples. We present previously unpublished filtered KAIT photometry of SN 2007J and unfiltered (similar to *R* band) KAIT photometry of SNe 2004cs, 2005P, and 2007J. We also present previously unpublished filtered CSP photometry of SNe 2008ae and 2009J, unpublished filtered CfA photometry of SNe 2011ay and 2012Z, and unpublished filtered CHASE photometry of SNe 2009J and 2011ce.

Unfiltered (as part of LOSS) and broadband *BVRI* photometry of several SNe was obtained using KAIT at Lick Observatory. The data were reduced using a mostly automated pipeline developed for KAIT images (Ganeshalingam et al. 2010). Images are bias-corrected and flatfielded at the telescope. Using galaxy templates obtained a year and a half after discovery, the data images are galaxy-subtracted to remove galaxy flux at the position of the SN. The flux of the SN and the local field star are measured using the point-spread function (PSF)

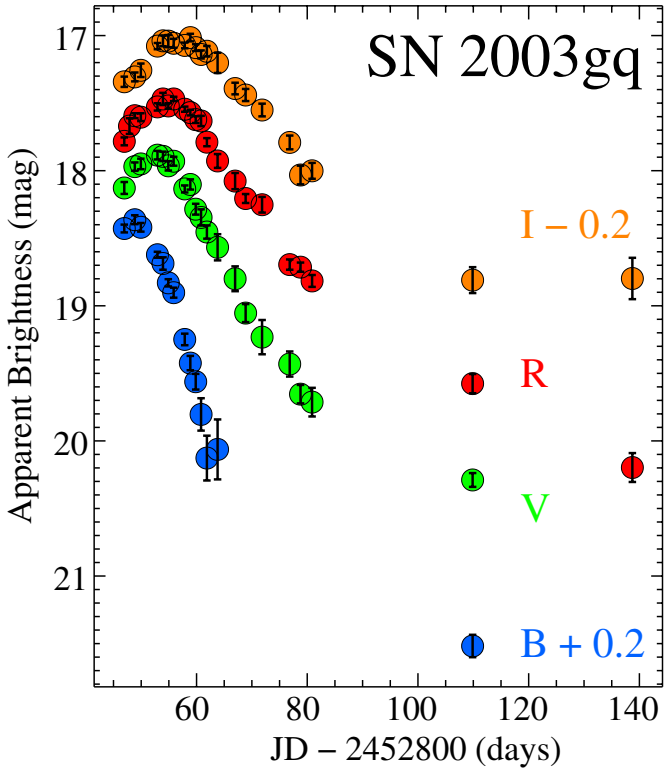


**Figure 10.** KAIT *BVRI* (blue, green, red, and orange, respectively) light curves of SN 2003gq (Ganeshalingam et al. 2010). The uncertainties for most data points are smaller than the plotted symbols.

(An extended and color version of this figure is available in the online journal.)

fitting photometry package DAOPHOT in IRAF.[17] Instrumental magnitudes are color-corrected to the Landolt (1992) system using the average color terms measured on multiple photometric nights.

The majority of the CSP imaging was obtained at the Las Campanas Observatory (LCO) with the Henrietta Swope 1.0 m telescope equipped with the "SITe3" direct optical camera. These data are accompanied with additional images taken with the Irénée du Pont 2.5 m telescope. Optical du Pont images were obtained with the direct CCD camera known as "Tek 5"; see Hamuy et al. (2006) for details regarding these instruments. An in-depth description of CSP observational procedures, data-reduction techniques, and the computation of definitive photometry in the natural photometric system is given by Contreras et al. (2010), with additional descriptions in Stritzinger et al. (2012). SN photometry is computed differentially with respect to a local sequence of stars, and reported in the natural system. Conversions to standard-system magnitudes are presented by Stritzinger et al. (2011).

Photometry of several SNe was also obtained by the 0.41 m Panchromatic Robotic Optical Monitoring and Polarimetry Telescope (PROMPT; Reichart et al. 2005). Instrumental magnitudes were measured using the template-subtraction technique with a code based on the ISIS package (Alard & Lupton 1998; Alard 2000), and we report magnitudes in the natural system.

All previously unpublished photometry is listed in Table 3. Light curves for SN 2003gq are shown in Figure 10. Light

[17] IRAF: The Image Reduction and Analysis Facility is distributed by the National Optical Astronomy Observatory, which is operated by the Association of Universities for Research in Astronomy (AURA) under cooperative agreement with the National Science Foundation (NSF).

**Table 3**
Photometry of SNe Iax

| JD − 2450000 | Magnitude | Uncertainty |
|---|---|---|
| SN 2004cs | | |
| KAIT Unfiltered | | |
| 3177.90 | 19.16 | 0.14 |
| 3179.90 | 18.11 | 0.04 |
| 3180.89 | 17.82 | 0.03 |
| 3182.89 | 17.60 | 0.03 |
| 3184.85 | 17.47 | 0.04 |
| 3187.87 | 17.54 | 0.05 |
| 3193.89 | 18.04 | 0.04 |
| 3195.81 | 18.18 | 0.04 |
| 3197.82 | 18.30 | 0.05 |
| 3199.82 | 18.65 | 0.06 |
| 3200.79 | 18.78 | 0.08 |
| 3204.86 | 18.88 | 0.20 |
| 3206.80 | 19.12 | 0.14 |
| SN 2005P | | |
| KAIT Unfiltered | | |
| 3392.05 | 17.93 | 0.09 |
| 3393.09 | 17.82 | 0.09 |
| 3394.07 | 17.88 | 0.09 |
| 3395.03 | 17.97 | 0.04 |
| 3412.03 | 18.28 | 0.12 |
| 3436.97 | 18.70 | 0.13 |
| 3445.98 | 18.78 | 0.15 |
| 3461.97 | 19.03 | 0.14 |
| 3471.93 | 18.91 | 0.31 |
| 3479.89 | 19.31 | 0.22 |
| SN 2007J | | |
| KAIT Unfiltered | | |
| 4115.75 | 18.56 | 0.05 |
| 4117.75 | 18.68 | 0.07 |
| 4118.75 | 18.95 | 0.06 |
| 4123.75 | 19.15 | 0.10 |
| KAIT *V* | | |
| 4123.66 | 19.63 | 0.11 |
| 4124.61 | 19.75 | 0.09 |
| 4125.62 | 19.89 | 0.64 |
| KAIT *R* | | |
| 4123.66 | 18.91 | 0.06 |
| 4124.61 | 19.01 | 0.06 |
| 4125.62 | 19.05 | 0.36 |
| 4133.69 | 19.29 | 0.14 |
| 4134.62 | 19.53 | 0.16 |
| 4135.64 | 19.51 | 0.15 |
| 4136.64 | 19.84 | 0.39 |
| 4137.62 | 19.61 | 0.14 |
| KAIT *I* | | |
| 4123.66 | 18.53 | 0.06 |
| 4124.61 | 18.50 | 0.09 |
| 4125.62 | 18.52 | 0.29 |
| 4133.69 | 18.66 | 0.14 |
| 4134.62 | 19.16 | 0.17 |
| 4135.64 | 19.08 | 0.16 |
| 4136.64 | 18.95 | 0.31 |
| 4137.62 | 18.95 | 0.14 |
| SN 2008ae | | |
| CSP *u* | | |
| 4508.75 | 19.34 | 0.04 |
| 4512.71 | 19.69 | 0.07 |
| 4515.71 | 20.34 | 0.41 |
| 4519.67 | 20.80 | 0.23 |
| CSP *B* | | |
| 4508.75 | 18.64 | 0.02 |
| 4512.71 | 18.73 | 0.02 |
| 4515.71 | 19.08 | 0.12 |
| 4519.67 | 19.67 | 0.05 |
| 4521.73 | 19.94 | 0.06 |
| 4523.69 | 20.21 | 0.06 |
| 4527.65 | 20.60 | 0.05 |
| 4532.64 | 21.17 | 0.09 |
| 4552.65 | 21.57 | 0.17 |
| 4558.58 | 21.76 | 0.11 |
| 4564.58 | 21.72 | 0.11 |
| 4591.54 | 22.21 | 0.17 |
| 4530.63 | 21.00 | 0.08 |
| 4538.62 | 21.51 | 0.12 |
| 4540.60 | 21.40 | 0.10 |
| CSP *V* | | |
| 4508.75 | 18.35 | 0.01 |
| 4512.71 | 18.19 | 0.01 |
| 4515.71 | 18.18 | 0.06 |
| 4519.67 | 18.37 | 0.02 |
| 4521.73 | 18.58 | 0.02 |
| 4523.69 | 18.72 | 0.02 |
| 4527.65 | 19.08 | 0.02 |
| 4532.64 | 19.53 | 0.03 |
| 4541.65 | 19.78 | 0.04 |
| 4547.65 | 20.07 | 0.10 |
| 4549.61 | 20.12 | 0.07 |
| 4552.65 | 20.18 | 0.05 |
| 4558.58 | 20.28 | 0.04 |
| 4564.58 | 20.36 | 0.04 |
| 4569.64 | 20.57 | 0.10 |
| 4574.56 | 20.46 | 0.13 |
| 4576.53 | 20.43 | 0.10 |
| 4591.54 | 20.92 | 0.07 |
| 4597.58 | 21.06 | 0.11 |
| 4530.63 | 19.33 | 0.02 |
| 4538.62 | 19.74 | 0.03 |
| 4540.60 | 19.80 | 0.03 |
| CSP *g* | | |
| 4508.75 | 18.44 | 0.01 |
| 4512.71 | 18.44 | 0.01 |
| 4515.71 | 18.70 | 0.04 |
| 4519.67 | 19.08 | 0.03 |
| 4521.73 | 19.32 | 0.03 |
| 4523.69 | 19.52 | 0.02 |
| 4527.65 | 20.00 | 0.03 |
| 4532.64 | 20.38 | 0.03 |
| 4541.65 | 20.88 | 0.09 |
| 4549.61 | 20.89 | 0.12 |
| 4552.65 | 21.07 | 0.09 |
| 4558.58 | 21.12 | 0.05 |
| 4564.58 | 21.17 | 0.05 |
| 4569.64 | 21.22 | 0.13 |
| 4591.54 | 21.62 | 0.07 |
| 4597.58 | 21.73 | 0.16 |
| 4530.63 | 20.28 | 0.03 |
| 4538.62 | 20.62 | 0.04 |
| 4540.60 | 20.80 | 0.04 |
| CSP *r* | | |
| 4508.75 | 18.16 | 0.01 |

**Table 3**
(Continued)

| JD − 2450000 | Magnitude | Uncertainty |
|---|---|---|
| 4512.71 | 17.94 | 0.01 |
| 4515.71 | 17.96 | 0.06 |
| 4519.67 | 17.95 | 0.01 |
| 4521.73 | 18.03 | 0.01 |
| 4523.69 | 18.14 | 0.01 |
| 4527.65 | 18.39 | 0.01 |
| 4532.64 | 18.73 | 0.01 |
| 4541.65 | 19.23 | 0.02 |
| 4547.65 | 19.42 | 0.04 |
| 4549.61 | 19.37 | 0.03 |
| 4552.65 | 19.55 | 0.03 |
| 4558.58 | 19.68 | 0.02 |
| 4564.58 | 19.84 | 0.03 |
| 4569.64 | 19.90 | 0.04 |
| 4574.56 | 20.02 | 0.06 |
| 4576.53 | 19.98 | 0.05 |
| 4591.54 | 20.43 | 0.04 |
| 4597.58 | 20.65 | 0.08 |
| 4530.63 | 18.62 | 0.01 |
| 4538.62 | 19.08 | 0.02 |
| 4540.60 | 19.19 | 0.02 |
| | CSP *i* | |
| 4508.75 | 18.26 | 0.01 |
| 4512.71 | 18.02 | 0.01 |
| 4515.71 | 17.88 | 0.05 |
| 4519.67 | 17.85 | 0.01 |
| 4521.73 | 17.91 | 0.01 |
| 4523.69 | 17.94 | 0.01 |
| 4527.65 | 18.11 | 0.01 |
| 4532.64 | 18.37 | 0.01 |
| 4541.65 | 18.84 | 0.02 |
| 4547.65 | 19.04 | 0.04 |
| 4549.61 | 19.09 | 0.03 |
| 4552.65 | 19.23 | 0.03 |
| 4558.58 | 19.35 | 0.03 |
| 4564.58 | 19.54 | 0.03 |
| 4569.64 | 19.56 | 0.04 |
| 4574.56 | 19.70 | 0.06 |
| 4576.53 | 19.70 | 0.05 |
| 4591.54 | 20.08 | 0.04 |
| 4597.58 | 20.25 | 0.08 |
| 4530.63 | 18.28 | 0.02 |
| 4538.62 | 18.70 | 0.01 |
| 4540.60 | 18.77 | 0.02 |
| | SN 2009J | |
| | CSP *u* | |
| 4848.71 | 19.64 | 0.06 |
| 4855.74 | 21.27 | 0.16 |
| 4856.70 | 21.62 | 0.30 |
| 4858.70 | 21.55 | 0.21 |
| 4859.73 | 22.27 | 0.51 |
| | CSP *B* | |
| 4848.72 | 18.97 | 0.02 |
| 4855.73 | 20.14 | 0.04 |
| 4856.71 | 20.28 | 0.04 |
| 4858.71 | 20.42 | 0.07 |
| 4859.74 | 20.67 | 0.06 |
| 4866.67 | 21.20 | 0.12 |
| 4867.69 | 21.39 | 0.14 |
| | CSP *V* | |
| 4848.71 | 18.71 | 0.02 |
| 4855.73 | 19.18 | 0.02 |
| 4856.70 | 19.28 | 0.02 |

**Table 3**
(Continued)

| JD − 2450000 | Magnitude | Uncertainty |
|---|---|---|
| 4858.71 | 19.41 | 0.03 |
| 4859.73 | 19.55 | 0.03 |
| 4866.67 | 19.93 | 0.04 |
| 4867.69 | 20.04 | 0.06 |
| | CSP *g* | |
| 4848.69 | 18.71 | 0.01 |
| 4855.75 | 19.60 | 0.02 |
| 4856.69 | 19.75 | 0.02 |
| 4858.69 | 19.86 | 0.03 |
| 4859.72 | 20.11 | 0.03 |
| 4866.65 | 20.52 | 0.06 |
| 4867.67 | 20.44 | 0.07 |
| | CSP *r* | |
| 4848.70 | 18.68 | 0.01 |
| 4855.75 | 18.85 | 0.01 |
| 4856.69 | 18.92 | 0.01 |
| 4858.69 | 19.07 | 0.02 |
| 4859.72 | 19.11 | 0.02 |
| 4866.65 | 19.55 | 0.02 |
| 4867.67 | 19.56 | 0.03 |
| | CSP *i* | |
| 4848.70 | 18.91 | 0.02 |
| 4855.76 | 18.89 | 0.02 |
| 4856.69 | 18.89 | 0.02 |
| 4858.70 | 19.04 | 0.03 |
| 4859.72 | 19.05 | 0.03 |
| 4866.66 | 19.52 | 0.03 |
| 4867.67 | 19.44 | 0.03 |
| | CHASE *R* | |
| 4840.60 | 19.34 | 0.21 |
| 4844.58 | 19.14 | 0.12 |
| 4845.56 | 19.06 | 0.09 |
| 4848.60 | 18.86 | 0.09 |
| 4858.59 | 19.21 | 0.10 |
| 4861.59 | 19.46 | 0.14 |
| 4886.63 | 20.35 | 0.33 |
| | SN 2011ay | |
| | CfA *B* | |
| 5645.61 | 17.11 | 0.10 |
| 5646.61 | 17.04 | 0.07 |
| 5647.64 | 17.04 | 0.07 |
| 5648.68 | 17.05 | 0.08 |
| 5665.63 | 18.88 | 0.33 |
| 5673.67 | 19.31 | 0.37 |
| 5674.65 | 19.00 | 0.49 |
| 5686.64 | 19.52 | 0.38 |
| 5689.66 | 19.46 | 0.49 |
| 5691.66 | 19.56 | 0.65 |
| 5692.69 | 19.38 | 0.33 |
| 5693.66 | 19.56 | 0.53 |
| | CfA *V* | |
| 5645.60 | 16.93 | 0.03 |
| 5646.60 | 16.80 | 0.04 |
| 5647.64 | 16.74 | 0.03 |
| 5648.67 | 16.70 | 0.04 |
| 5665.62 | 17.34 | 0.09 |
| 5673.66 | 17.77 | 0.09 |
| 5674.65 | 17.86 | 0.14 |
| 5686.63 | 18.30 | 0.12 |
| 5689.66 | 18.37 | 0.16 |
| 5691.66 | 18.25 | 0.15 |

**Table 3**
(Continued)

| JD − 2450000 | Magnitude | Uncertainty |
|---|---|---|
| 5692.68 | 18.45 | 0.17 |
| 5693.66 | 18.41 | 0.17 |
| 5698.66 | 18.79 | 0.26 |
| | CfA *r* | |
| 5647.63 | 16.62 | 0.04 |
| 5648.67 | 16.64 | 0.03 |
| 5665.62 | 16.77 | 0.06 |
| 5670.64 | 17.12 | 0.06 |
| 5673.66 | 17.29 | 0.15 |
| 5674.64 | 17.39 | 0.10 |
| 5686.63 | 17.84 | 0.11 |
| 5689.66 | 17.89 | 0.18 |
| 5691.66 | 17.71 | 0.18 |
| 5692.68 | 18.00 | 0.21 |
| 5693.66 | 18.04 | 0.17 |
| 5698.65 | 18.31 | 0.28 |
| | CfA *i* | |
| 5647.64 | 16.78 | 0.30 |
| 5648.67 | 16.97 | 0.27 |
| 5665.62 | 16.84 | 0.27 |
| 5670.64 | 17.30 | 0.24 |
| 5673.66 | 17.29 | 0.34 |
| 5674.64 | 17.36 | 0.31 |
| 5686.63 | 18.12 | 0.67 |
| 5689.65 | 18.14 | 0.53 |
| 5691.66 | 18.19 | 0.32 |
| 5692.68 | 18.31 | 1.06 |
| 5693.65 | 18.29 | 0.40 |
| 5698.65 | 18.56 | 0.51 |
| 5852.98 | 20.20 | 0.36 |
| 5855.95 | 20.24 | 0.33 |
| | SN 2012Z | |
| | CfA *B* | |
| 5969.61 | 14.73 | 0.01 |
| 5977.62 | 15.43 | 0.01 |
| 5978.64 | 15.55 | 0.01 |
| | CfA *V* | |
| 5969.60 | 14.48 | 0.01 |
| 5977.62 | 14.52 | 0.01 |
| 5978.64 | 14.60 | 0.01 |
| 5992.62 | 15.61 | 0.01 |
| | CfA *r* | |
| 5969.60 | 14.39 | 0.01 |
| 5977.61 | 14.29 | 0.01 |
| 5978.63 | 14.33 | 0.01 |
| 5992.62 | 15.03 | 0.01 |
| 5994.60 | 15.15 | 0.01 |
| | CfA *i* | |
| 5969.60 | 14.56 | 0.01 |
| 5977.61 | 14.38 | 0.01 |
| 5978.63 | 14.37 | 0.01 |
| 5992.61 | 14.88 | 0.01 |
| 5994.60 | 14.98 | 0.01 |
| | SN 2011ce | |
| | CHASE Unfiltered | |
| 5646.86 | 17.40 | 0.09 |
| 5670.90 | 16.86 | 0.05 |
| 5671.82 | 16.90 | 0.05 |
| 5699.81 | 17.95 | 0.09 |

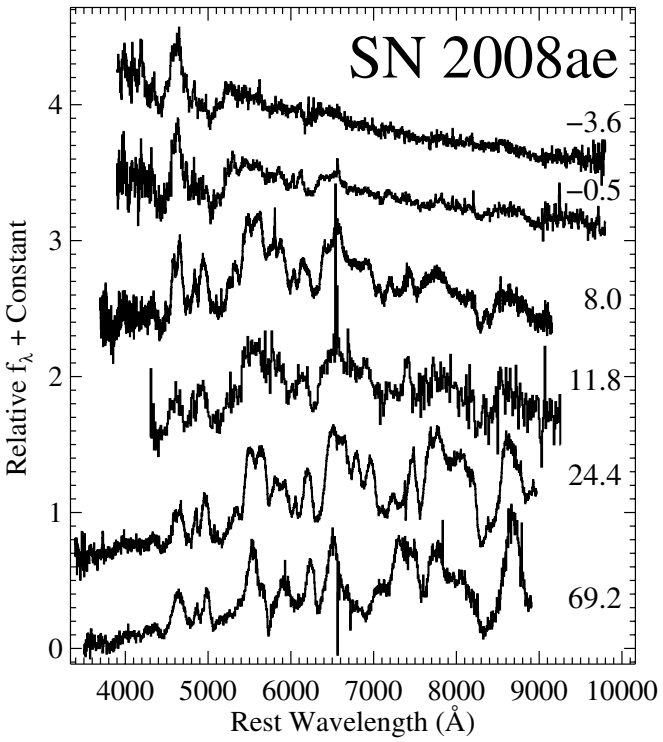


**Figure 11.** Optical spectra of SN 2008ae. Rest-frame phases relative to *V* maximum are listed to the right of each spectrum.

curves for SNe 2004cs, 2005P, 2005cc, 2006hn, 2007J, 2008ae, 2009J, 2011ay, and 2012Z are available in the online version of this manuscript.

### *3.2. Spectroscopy*

We have obtained several low-resolution optical spectra with the FAST spectrograph (Fabricant et al. 1998) on the FLWO 1.5 m telescope, the Kast double spectrograph (Miller & Stone 1993) on the Shane 3 m telescope at Lick Observatory, the EMMI spectrograph (Dekker et al. 1986) on the New Technology Telescope at La Silla Observatory, the EFOSC spectrograph (Buzzoni et al. 1984) on the ESO 3.6 m telescope, the LDSS3 spectrograph[18] on the Magellan Clay 6.5 m telescope, the IMACS spectrograph (Dressler et al. 2011) on the Magellan Baade 6.5 m telescope, and the Low Resolution Imaging Spectrometer (LRIS; Oke et al. 1995) on the 10 m Keck I telescope.

Standard CCD processing and spectrum extraction were accomplished with IRAF. The data were extracted using the optimal algorithm of Horne (1986). Low-order polynomial fits to calibration-lamp spectra were used to establish the wavelength scale, and small adjustments derived from night-sky lines in the object frames were applied. We employed our own IDL routines to flux calibrate the data and remove telluric lines using the well-exposed continua of the spectrophotometric standard stars (Wade & Horne 1988; Foley et al. 2003). Details of our spectroscopic reduction techniques are described by Silverman et al. (2012).

A log of all previously unpublished spectral observations is presented in Table 4. Spectral sequences for SNe 2008ae, 2009J, 2011ay, and 2012Z are shown in Figures 11–14. We only display previously unpublished data. We do not display our single previously unpublished spectrum of SN 2008ge since

[18] http://www.lco.cl/telescopes-information/magellan/instruments/ldss-3.

**Table 4**
Log of Spectral Observations

| Phase[a] | UT Date | Telescope/ Instrument | Exp. (s) | Observer[b] |
|---|---|---|---|---|
| | | SN 2007J | | |
| 2–42 | 2007 Jan 17.2 | FLWO/FAST | 1800 | PB1 |
| 6–46 | 2007 Jan 21.3 | Lick/Kast | 2100 | MG, TS |
| 6–46 | 2007 Jan 21.4 | Keck/LRIS | 300 | AF, JS, RF |
| 30–70 | 2007 Feb 14.3 | Keck/LRIS | 1200 | AF, JS, RC, RF |
| 62–102 | 2007 Mar 18.3 | Keck/LRIS | 900 | JS, RC |
| | | SN 2008ae | | |
| −3.6 | 2008 Feb 13.3 | NTT/EMMI | 900 | GF |
| −0.5 | 2008 Feb 16.4 | Lick/Kast | 1800 | JS, MG, NL, TS |
| 8.0 | 2008 Feb 25.3 | Clay/LDSS | 1800 | GP, NM |
| 11.8 | 2008 Feb 29.2 | Lick/Kast | 1800 | JS, MG, NL, TS |
| 24.4 | 2008 Mar 13.1 | ESO/EFOSC | 1200 | GF |
| 69.2 | 2008 Apr 28.3 | Keck/LRIS | 900 | AF, DP, JS, TS |
| | | SN 2008ge | | |
| 41.1 | 2008 Oct 27.5 | Keck/LRIS | 105 | AF, BT, JS, TS |
| | | SN 2009J | | |
| 0.2 | 2009 Jan 17.2 | Clay/LDSS | 700 | MP, MS |
| 5.2 | 2009 Jan 22.2 | Clay/LDSS | 700 | NM |
| 21.8 | 2009 Feb 8.1 | Clay/LDSS | 700 | NM |
| 22.9 | 2009 Feb 9.2 | Clay/LDSS | 700 | NM |
| 24.7 | 2009 Feb 11.1 | Baade/IMACS | 600 | NM |
| 57.2 | 2009 Mar 16.1 | Baade/IMACS | 1200 | NM |
| | | SN 2010ae | | |
| ... | 2010 Feb 26.1 | Baade/IMACS | 1800 | AS1 |
| | | SN 2011ay | | |
| −2.0 | 2008 Mar 29.2 | Lick/Kast | 1500 | AB, JW, RA |
| 1.9 | 2008 Apr 2.2 | Lick/Kast | 1921 | SH |
| 4.8 | 2008 Apr 5.2 | Lick/Kast | 2100 | JR, KC |
| 10.8 | 2008 Apr 11.2 | Lick/Kast | 1800 | AS2, SH |
| 26.4 | 2008 Apr 27.2 | Lick/Kast | 1800 | VB |
| 36.2 | 2008 May 7.2 | Lick/Kast | 1800 | RA |
| 49.9 | 2008 May 21.2 | Lick/Kast | 2100 | AD, GC, ML |
| 62.7 | 2008 Jun 3.2 | Keck/LRIS | 450 | AF, BC, JS |
| 175.6 | 2008 Sep 26.6 | Keck/LRIS | 1850 | AF, BC, JS |
| | | SN 2011ce | | |
| 42[c] | 2011 Apr 24.2 | Baade/IMACS | 450 | JA |
| 371[c] | 2012 Apr 20.4 | Baade/IMACS | 3600 | RF |
| | | SN 2012Z | | |
| −13.7 | 2012 Feb 1.2 | Lick/Kast | 842 | BC, DC |
| −12.7 | 2012 Feb 2.2 | Lick/Kast | 2400 | KC, PB2 |
| 1.1 | 2012 Feb 16.1 | FLWO/FAST | 1800 | JI |
| 4.1 | 2012 Feb 19.1 | FLWO/FAST | 1800 | JI |
| 6.1 | 2012 Feb 21.1 | FLWO/FAST | 1800 | JI |
| 6.2 | 2012 Feb 21.3 | Keck/LRIS | 300 | AM1, AM2, JS, PN |
| 7.1 | 2012 Feb 22.1 | FLWO/FAST | 1800 | JI |
| 29.0 | 2012 Mar 15.2 | Keck/LRIS | 510 | AM1, BC, JS, PN |

**Notes.**
[a] Rest-frame days since $V$ maximum.
[b] AB = A. Barth, AD = A. Diamond-Stanic, AF = A. Filippenko, AM1 = A. Miller, AM1 = A. Morgan, AS1 = A. Soderberg, AS2 = A. Sonnenfeld, BC = B. Cenko, BT = B. Tucker, DC = D. Cohen, DP = D. Poznanski, GC = G. Canalizo, GF = G. Folatelli, GP = G. Pignata, JA = J. Anderson, JI = J. Irwin, JR = J. Rex, JS = J. Silverman, JW = J. Walsh, KC = K. Clubb, MG = M. Ganeshalingam, ML = M. Lazarova, MP = M. Phillips, MS = M. Stritzinger, NL = N. Lee, NM = N. Morrell, PB1 = P. Berlind, PB2 = P. Blanchard, PN = P. Nugent, RA = R. Assef, RC = R. Chornock, RF = R. Foley, SH = S. Hoenig, TS = T. Steele, VB = V. Bennert.
[c] Approximate phase; see Section 2.24 for details.

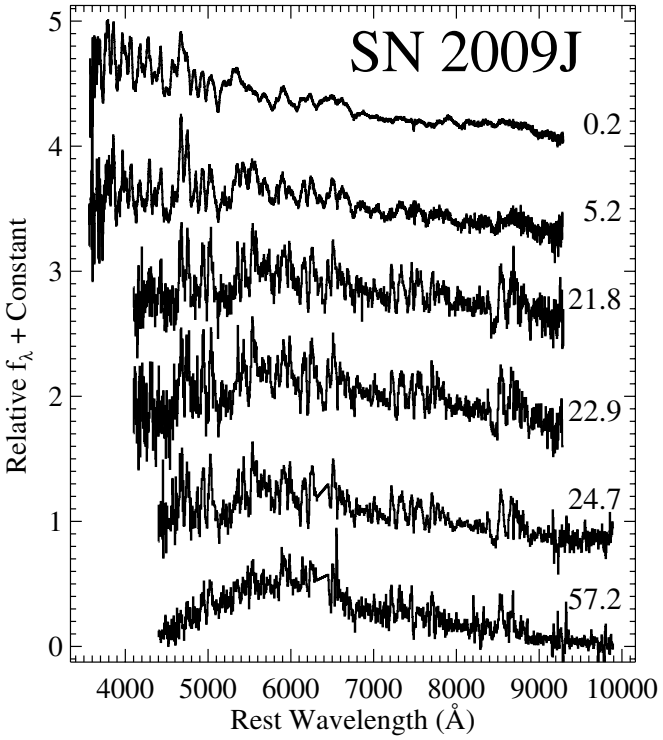


**Figure 12.** Optical spectra of SN 2009J. Rest-frame phases relative to $V$ maximum are listed to the right of each spectrum.

it was obtained the same night as the first spectrum presented by Foley et al. (2010c).

## 4. PHOTOMETRIC PROPERTIES

In this section, we examine the photometric properties of SNe Iax. A minority of the full sample has filtered photometry that covers maximum brightness. Since observations near maximum brightness are critical for direct comparisons between SNe, we focus on the SNe having those data. For the SNe in our sample with light curves around maximum brightness, we can derive several light curve parameters: time of maximum brightness, peak brightness, peak absolute brightness, and decline rate. We fit low-order polynomials to each light curve near maximum brightness to derive these values for each available band. For some SNe and some bands, we can only place limits or broad ranges on the derived values. We present our measurements in Table 5.

### *4.1. Photometric Relations*

Using the measured times of maximum, we can directly compare the absolute-magnitude light curves of several SNe in the class. We present those light curves in Figure 15 and note that they have not been corrected for host-galaxy extinction (see Section 4.2). The figure shows the large range of peak absolute magnitudes for the class. It also displays the differing photometric behavior. Some SNe with very similar absolute magnitudes can have very different decline rates (e.g., SNe 2002cx and 2008ge[19]). Despite these outliers, there is a general trend that the more luminous SNe at peak tend to have

[19] The SN 2008ge light curve presented by Foley et al. (2010c). was observed unfiltered and converted to $V$, and therefore some of the discrepancy may be related to the slightly different bandpasses.

**Table 5**
Light-curve Properties of SNe Iax

| SN Name | $B$ (mag) | $V$ (mag) | $R$ (mag) | $I$ (mag) | $g$ (mag) | $r$ (mag) | $i$ (mag) |
|---|---|---|---|---|---|---|---|
| | | | $t_{max}$ (JD − 2,450,000) | | | | |
| 2002cx | 2413.34 (0.25) | 2418.31 (0.39) | 2420.95 (0.94) | 2421.79 (2.83) | ... | ... | ... |
| 2003gq | 2848.78 (0.26) | 2852.56 (0.28) | 2854.49 (0.35) | 2857.01 (0.40) | ... | ... | ... |
| 2005cc | <3519.29 | 3522.10 (0.18) | 3523.01 (0.11) | 3526.88 (0.30) | ... | ... | ... |
| 2005hk | 3685.09 (0.44) | 3689.81 (0.63) | 3690.04 (1.93) | 3694.86 (0.27) | 3685.48 (0.74) | 3691.61 (0.27) | 3694.52 (0.47) |
| 2007qd | ... | ... | ... | ... | 4355.42–4405.89 | 4355.42–4405.89 | 4355.42–4405.89 |
| 2008A | 4478.23 (0.23) | 4483.61 (0.31) | 4485.03 (0.36) | 4488.28 (0.54) | ... | 4483.15 (1.69) | 4485.67 (1.67) |
| 2008ae | 4508.40 (1.71) | 4513.52 (0.11) | ... | ... | ... | 4515.73 (0.53) | 4518.30 (0.71) |
| 2008ge | ... | 4725.77 (1.69) | ... | ... | ... | ... | ... |
| 2008ha | 4783.23 (0.16) | 4785.24 (0.30) | 4787.30 (0.18) | 4787.95 (0.28) | ... | ... | ... |
| 20009J | <4848.72 | <4848.71 | 4850.03 (1.45) | ... | <4848.69 | <4848.70 | 4852.39 (2.43) |
| 2009ku | ... | ... | ... | ... | 5097.87 (0.59) | 5098.33 (0.88) | 5099.54 (1.70) |
| 2011ay | 5647.64 (1.54) | 5651.81 (1.70) | ... | ... | ... | 5653.77 (1.53) | 5653.12 (4.96) |
| 2012Z | <5969.61 | $\lesssim$5969.60 | ... | ... | ... | 5974.91 (0.78) | 5977.27 (1.89) |
| | | | Peak Magnitude | | | | |
| 2002cx | 17.78 (0.23) | 17.72 (0.09) | 17.58 (0.02) | 17.42 (0.19) | ... | ... | ... |
| 2003gq | 18.19 (0.01) | 17.88 (0.01) | 17.48 (0.02) | 17.25 (0.01) | ... | ... | ... |
| 2005cc | <16.70 | 16.27 (0.01) | 15.92 (0.01) | 15.68 (0.01) | ... | ... | ... |
| 2005hk | 15.92 (0.01) | 15.73 (0.01) | 15.51 (0.01) | 15.37 (0.01) | 15.80 (0.03) | 15.67 (0.01) | 15.79 (0.01) |
| 2007qd | ... | ... | ... | ... | <21.90 | <21.72 | <21.35 |
| 2008A | 16.39 (0.01) | 16.11 (0.01) | 15.82 (0.01) | 15.67 (0.01) | ... | 16.01 (0.02) | 16.06 (0.02) |
| 2008ae | 18.62 (0.03) | 18.17 (0.02) | ... | ... | ... | 17.93 (0.05) | 17.85 (0.02) |
| 2008ge | ... | 13.77 (0.12) | ... | ... | ... | ... | ... |
| 2008ha | 18.23 (0.01) | 17.68 (0.01) | 17.54 (0.01) | 17.36 (0.01) | ... | ... | ... |
| 2009J | <18.97 | <18.72 | 18.90 (0.16) | ... | <18.71 | <18.68 | 18.79 (0.09) |
| 2009ku | ... | ... | ... | ... | 19.60 (0.01) | 19.26 (0.01) | 19.24 (0.01) |
| 2011ay | 17.04 (0.01) | 16.62 (0.04) | ... | ... | ... | 16.54 (0.11) | 16.83 (0.11) |
| 2012Z | <14.73 | $\lesssim$14.48 | ... | ... | ... | 14.27 (0.03) | 14.27 (0.11) |
| | | | Peak Absolute Magnitude | | | | |
| 2002cx | −17.48 (0.28) | −17.52 (0.18) | −17.64 (0.15) | −17.77 (0.15) | ... | ... | ... |
| 2003gq | −16.76 (0.15) | −17.01 (0.15) | −17.37 (0.15) | −17.56 (0.15) | ... | ... | ... |
| 2005cc | <−16.05 | −16.79 (0.15) | −17.13 (0.15) | −17.38 (0.15) | ... | ... | ... |
| 2005hk | −17.69 (0.15) | −17.86 (0.15) | −18.07 (0.15) | −18.19 (0.15) | −18.12 (0.36) | −17.91 (0.15) | −17.78 (0.15) |
| 2007qd | ... | ... | ... | ... | <−14.50 | <−14.61 | <−14.99 |
| 2008A | −17.92 (0.15) | −18.16 (0.15) | −18.41 (0.15) | −18.53 (0.15) | ... | −18.23 (0.15) | −18.15 (0.15) |
| 2008ae | −17.10 (0.15) | −17.53 (0.15) | ... | ... | ... | −17.76 (0.16) | −17.82 (0.15) |
| 2008ge | ... | −17.60 (0.25) | ... | ... | ... | ... | ... |
| 2008ha | −13.70 (0.15) | −14.18 (0.15) | −14.28 (0.15) | −14.41 (0.15) | ... | ... | ... |
| 2009J | <−15.53 | <−15.70 | −15.47 (0.22) | ... | <−15.71 | <−15.70 | −15.54 (0.17) |
| 2009ku | ... | ... | ... | ... | −18.36 (0.15) | −18.70 (0.15) | −18.71 (0.15) |
| 2011ay | −18.05 (0.15) | −18.40 (0.16) | ... | ... | ... | −18.43 (0.19) | −18.10 (0.19) |
| 2012Z | <−17.96 | $\lesssim$−18.18 | ... | ... | ... | −18.37 (0.09) | −18.25 (0.14) |
| | | | $\Delta m_{15}$ (mag) | | | | |
| 2002cx | 1.23 (0.06) | 0.84 (0.09) | 0.54 (0.06) | 0.38 (0.06) | ... | ... | ... |
| 2003gq | 1.83 (0.02) | 0.98 (0.03) | 0.71 (0.10) | 0.52 (0.04) | ... | ... | ... |
| 2005cc | ... | 0.97 (0.01) | 0.65 (0.01) | 0.61 (0.06) | ... | ... | ... |
| 2005hk | 1.54 (0.05) | 0.92 (0.01) | 0.52 (0.13) | 0.52 (0.01) | 1.22 (0.15) | 0.67 (0.01) | 0.56 (0.03) |
| 2008A | 1.26 (0.07) | 0.82 (0.06) | 0.51 (0.01) | 0.38 (0.03) | ... | 0.56 (0.05) | 0.47 (0.03) |
| 2008ae | 1.35 (0.23) | 0.94 (0.02) | ... | ... | ... | 0.71 (0.13) | 0.50 (0.03) |
| 2008ge | ... | 0.34 (0.24) | ... | ... | ... | ... | ... |
| 2008ha | 2.17 (0.02) | 1.22 (0.03) | 0.97 (0.02) | 0.65 (0.02) | ... | ... | ... |
| 2009J | ... | ... | 0.79 (0.05) | ... | ... | ... | 0.69 (0.10) |
| 2009ku | ... | ... | ... | ... | 0.43 (0.08) | 0.25 (0.03) | 0.18 (0.09) |
| 2011ay | 1.34 (0.42) | 0.75 (0.12) | ... | ... | ... | 0.44 (0.14) | 0.26 (0.16) |
| 2012Z | ... | ... | ... | ... | ... | 0.59 (0.01) | 0.48 (0.11) |

broader light curves. There is also some diversity in the rise times (although most SNe have scarce pre-maximum data). Contrary to the trend seen with SNe Ia, SN 2008A is brighter than SN 2005hk but has a slightly shorter rise time. Nonetheless, the faintest SNe Iax, such as SN 2008ha and SN 2004cs, have shorter rise times and faster decline rates than the brightest SNe, such as SNe 2005hk and 2008A.

SNe Iax span a range of decline rates that is similar to that of normal SNe Ia, although the SN Iax range is somewhat larger. The rise-time range for SNe Iax (from SN 2008ha at ∼10 days

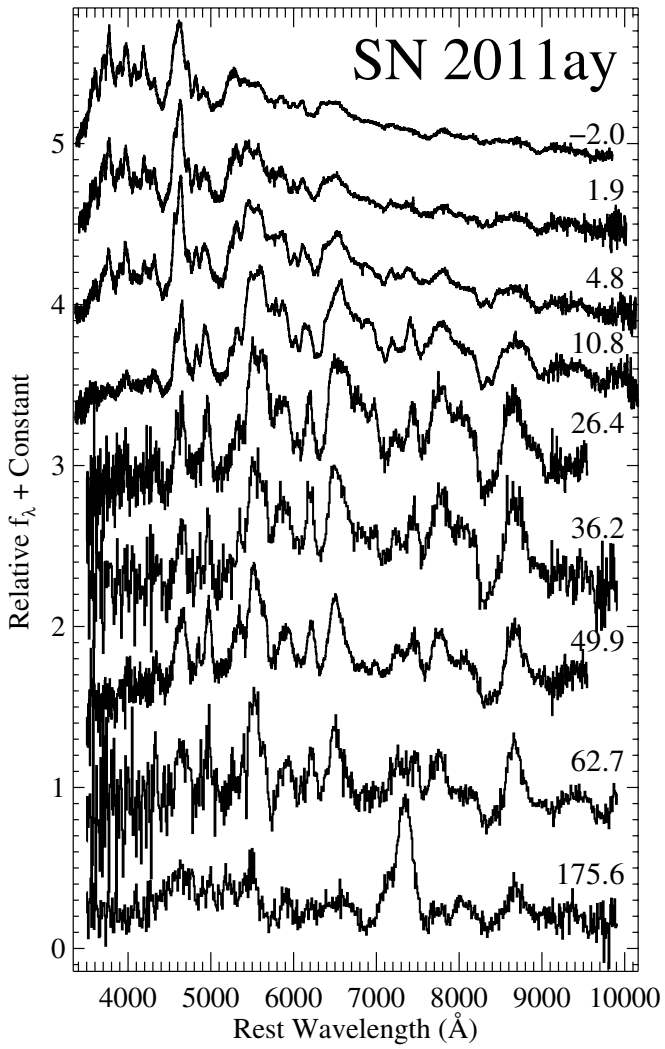


**Figure 13.** Optical spectra of SN 2011ay. Rest-frame phases relative to *V* maximum are listed to the right of each spectrum.

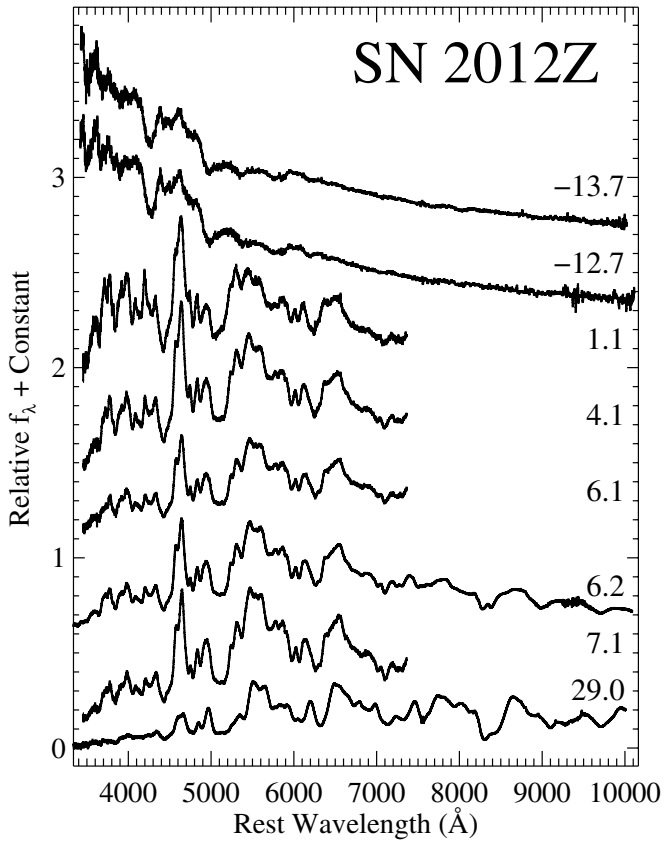


**Figure 14.** Optical spectra of SN 2012Z. Rest-frame phases relative to *V* maximum are listed to the right of each spectrum.

to SN 2008ge, which might be >20 days) is also larger than for that of SNe Ia (Ganeshalingam et al. 2011); based on current data, it appears that the average SN Iax has a shorter rise time than the average SN Ia, but few SNe have light curves sufficient for this measurement. Despite their rough similarity in light-curve shape, SNe Iax have consistently lower luminosity (even if that criterion is relaxed from our classification scheme) than SNe Ia.

For SNe Iax, there are several clear trends in the derived photometric parameters. Peak brightness and decline rates are highly correlated for a given object in all bands. In other words, an SN that is bright and declines slowly in *B* is also bright and declines slowly in *R*.

Performing a Bayesian Monte-Carlo linear regression on the data (Kelly 2007), we determine correlations between different parameters in different bands. The linear relationships and their correlation coefficients are presented in Table 6, where the equations are all of the form

$$p_2 = \alpha p_1 + \beta, \quad (1)$$

where $p_1$ and $p_2$ are the two parameters, $\alpha$ is the slope, and $\beta$ is the offset.

Using the equations in Table 6, one can effectively transform observations in one band into measurements in another.

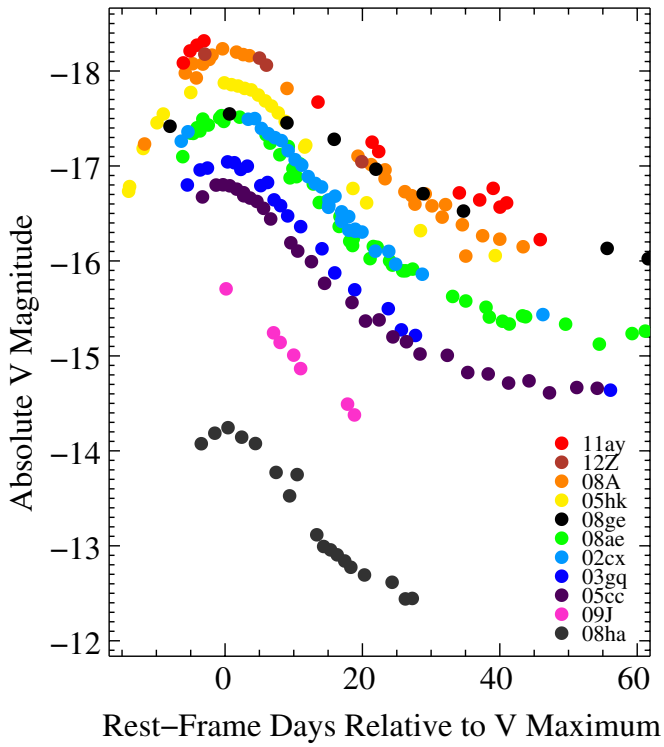


**Figure 15.** Absolute *V*-band light curves for a subset of SNe Iax. Each SN is plotted with a different color.

(A color version of this figure is available in the online journal.)

**Table 6**
Light-curve Relations for SNe Iax

| 1st Parameter | 2nd Parameter | Slope ($\alpha$) | Offset ($\beta$) | Equation No. | No. SNe | Correlation Coefficient |
|---|---|---|---|---|---|---|
| $t_{max}(B)$ | $t_{max}(V)$ | 0.98 (0.03) | 5.17 (1.83) | 2 | 7 | 0.9994 |
| $t_{max}(R)$ | $t_{max}(V)$ | 1.00 (0.02) | −1.47 (1.52) | 3 | 6 | 0.9997 |
| $t_{max}(I)$ | $t_{max}(V)$ | 1.00 (0.04) | −4.41 (2.79) | 4 | 6 | 0.9996 |
| $t_{max}(r)$ | $t_{max}(V)$ | ... | ... | ... | 4 | 0.958 |
| $t_{max}(i)$ | $t_{max}(V)$ | ... | ... | ... | 4 | 0.947 |
| $\Delta m_{15}(B)$ | $\Delta m_{15}(V)$ | 0.40 (0.12) | 0.32 (0.20) | 5 | 7 | 0.959 |
| $\Delta m_{15}(R)$ | $\Delta m_{15}(V)$ | 0.77 (0.26) | 0.46 (0.18) | 6 | 6 | 0.966 |
| $0\Delta m_{15}(I)$ | $\Delta m_{15}(V)$ | 1.35 (0.66) | 0.27 (0.34) | 7 | 6 | 0.929 |
| $\Delta m_{15}(r)$ | $\Delta m_{15}(V)$ | ... | ... | ... | 4 | −0.277 |
| $\Delta m_{15}(i)$ | $\Delta m_{15}(V)$ | ... | ... | ... | 4 | 0.471 |
| $M_B$ | $M_V$ | 0.95 (0.09) | −1.22 (1.45) | 8 | 7 | 0.996 |
| $M_R$ | $M_V$ | 0.96 (0.10) | −0.37 (1.74) | 9 | 6 | 0.997 |
| $M_I$ | $M_V$ | 0.97 (0.12) | −0.09 (2.13) | 10 | 6 | 0.992 |
| $M_r$ | $M_V$ | ... | ... | ... | 4 | −0.310 |
| $M_i$ | $M_V$ | ... | ... | ... | 4 | −0.311 |
| $\Delta m_{15}(V)$ | $M_V$ | 10.7 (2.4) | −27.4 (2.3) | 11 | 9 | 0.980 |
| $\Delta m_{15}(R)$ | $M_V$ | 8.3 (2.0) | −22.3 (1.3) | 12 | 6 | 0.982 |

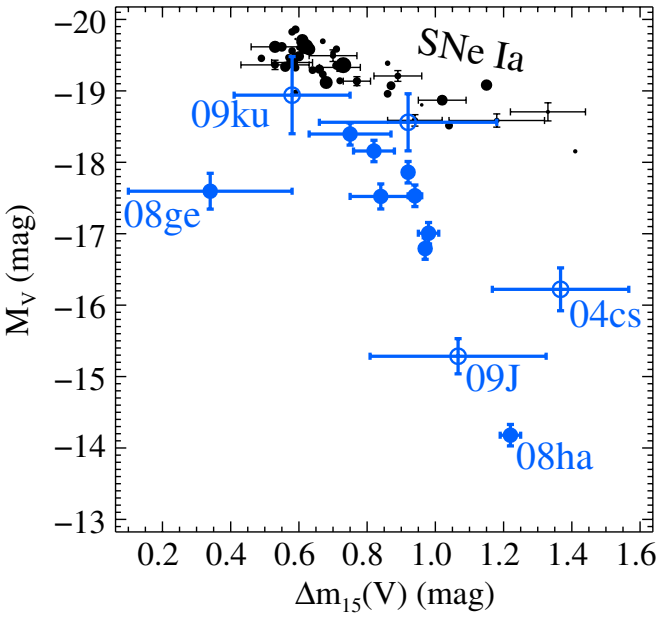


**Figure 16.** WLR ($\Delta m_{15}(V)$ vs. $M_V$) for SNe Ia (black points) and SNe Iax (blue points). Filled points are direct measurements in $V$, while the open points (SNe 2004cs, 2009J, and 2009ku) are an estimate by converting parameters measured from unfiltered (assumed to be $R$) or $r$ and $i$ to $V$. The sizes of the SN Ia points are inversely proportional to their uncertainty, with some points having representative errors bars to show the scaling.

(A color version of this figure is available in the online journal.)

However, we note that although the correlations are generally quite strong, the uncertainties for the linear relations are relatively large for several relations.

There are only four SNe with $V$ and $r/i$ light curves. The small number of measurements prevents robust determinations of relationships between the parameters in $V$ and $r/i$. However, the measurements in $r/i$ are consistent with measurements in $R/I$ (modulo offsets related to the filter response functions). As such, we are able to use the rough relations between $r/i$ and $V$ to estimate light-curve parameters in $V$ for SN 2009ku (which was only observed in PS1 bands). Doing this, we find $M_V = -18.94 \pm 0.54$ mag, and $\Delta m_{15}(V) = 0.58 \pm 0.17$ mag. Both values are consistent with those found by Narayan et al. (2011), who used only SN 2005hk to provide scalings. Using the same relations for SN 2012Z, we find $M_V = -18.56 \pm 0.40$ mag, which is consistent with the direct measurement in the $V$ band of $M_V \lesssim -18.18$ mag, and $\Delta m_{15}(V) = 0.92 \pm 0.26$ mag. We also convert the parameters measured for the unfiltered light curve of SN 2004cs assuming that the unfiltered light curve is equivalent to $R$. This conversion provides an estimate of $M_V = -16.2 \pm 0.3$ mag, and $\Delta m_{15}(V) = 1.4 \pm 0.2$ mag for SN 2004cs.

There is a clear progression in time of maximum brightness from blue to red, with the $VRI$ bands peaking 5.1, 6.6, and 11.1 days after $B$, respectively. This progression is similar to that seen for normal SNe I and is indicative of the SN ejecta cooling with time. There is no robust correlation between the time between maxima and light-curve shape.

In Figure 16, we show the relation between $\Delta m_{15}(V)$ and $M_V$ (uncorrected for host-galaxy extinction) for the nine SNe with measurements of these parameters and three SNe with estimates of these parameters. There is a general WLR, which is confirmed by a linear relationship between the parameters (Equation (11), which did not include the estimates for SNe 2004cs, 2009J, or 2009ku). The tight WLR for SNe Ia is interpreted as the result of a homogeneous class of objects with a single parameter (related to the $^{56}$Ni mass) controlling multiple observables (e.g., Mazzali et al. 2007). Similar physics may be behind the SN Iax WLR, but the large scatter indicates that the class is not as homogeneous as SNe Ia, with other parameters (perhaps ejecta mass; see Section 5.1) also being important.

We note that there is a strong correlation between $\Delta m_{15}(R)$ and $M_V$ (uncorrected for host-galaxy extinction) for our small sample. Narayan et al. (2011) found no strong correlation between these two quantities using a slightly different sample, but this appears to be because they included SN 2007qd in the relation. Although McClelland et al. (2010) reported peak magnitudes and decline rates for SN 2007qd (which were reproduced by Narayan et al. 2011), their light curves do not include any pre-maximum detections; consequently, their derived quantities may be misestimated. Using the McClelland et al. (2010) light curves, we present limits for SN 2007qd in Table 5.

The basic parameters of time of maximum, peak absolute magnitude, and light-curve shape for the SNe with $V$-band light curves are reported in Table 2. We also give estimates for SNe where we have light curves in bands other than $V$. Finally, we use the information in the discovery reports (combined with the relations presented above) to place approximate limits on $M_V$ at peak and $t_{max}(V)$.

### 4.2. Color Curves and Host-galaxy Reddening

In Figure 17, we present color curves for a subset of the class. The SNe all display the same general color evolution with time. SNe Iax typically get redder from maximum brightness until 15–20 days after maximum, at which point they stay relatively constant in color, but become slightly bluer with time.

Similar to what has been done for SNe Ia (Lira et al. 1998), we can create a tight color locus in $V-I$ and a relatively tight locus in $V-R$ when we assume some host-galaxy extinction. We find that reddening corrections corresponding to $E(B-V) = 0.05$, 0.4, 0.4, 0, 0.2, and 0.1 mag for SNe 2002cx, 2003gq, 2005cc, 2005hk, 2008A, and 2008ha, respectively, significantly reduce

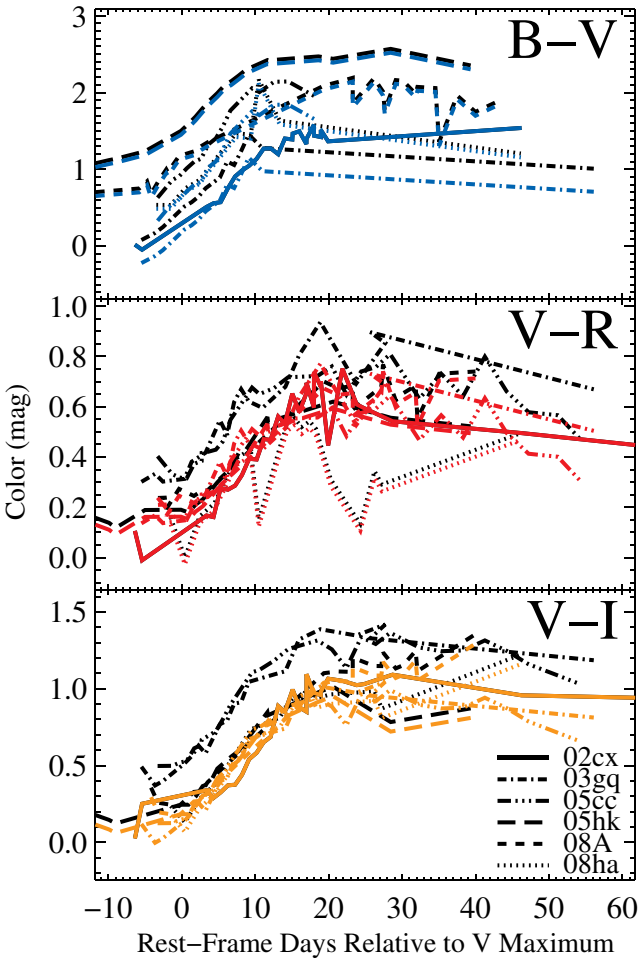


**Figure 17.** Color curves ($B-V$, $V-R$, and $V-I$ from top to bottom) of SNe Iax. The black lines correspond to the observed (corrected for Milky Way reddening) colors, while the colored curves correspond to an additional reddening correction corresponding to $E(B-V) = 0.05$, 0.4, 0.4, 0, 0.2, and 0.1 mag for SNe 2002cx, 2003gq, 2005cc, 2005hk, 2008A, and 2008ha, respectively.

(A color version of this figure is available in the online journal.)

the scatter in the $V-R$ and $V-I$ colors at all times. These corrections, however, do not improve the $B-V$ scatter, which remains quite large. It is therefore unclear if this color shift is related to dust reddening, or if the scatter is intrinsic to the SNe. We therefore do not apply these corrections to any of our estimates for the absolute magnitudes presented in Table 5. Furthermore, no dust reddening correction can simultaneously make the $V-R$ and $V-I$ colors of SN 2008ha similar to those of the other SNe; it is consistently bluer than all other SNe in $V-R$ when matching the $V-I$ color.

## 5. SPECTROSCOPIC PROPERTIES

### 5.1. Maximum-light Spectra

SNe Iax have a large range of photospheric velocities. For the members with spectra near $t = -2$ days relative to $V$ maximum, we show their spectra in Figure 18. The spectra are ordered by Si II λ6355 velocity, and the Si II λ6355 feature is shown in detail in the right panel of the figure. The spectra are at slightly different phases (from $t = -5.9$ to $-0.1$ days), so the comparison is appropriate for general patterns rather than looking for specific differences. Despite the different ejecta velocities, the spectra look very similar — the main differences are that the lower-velocity SNe have otherwise blended features

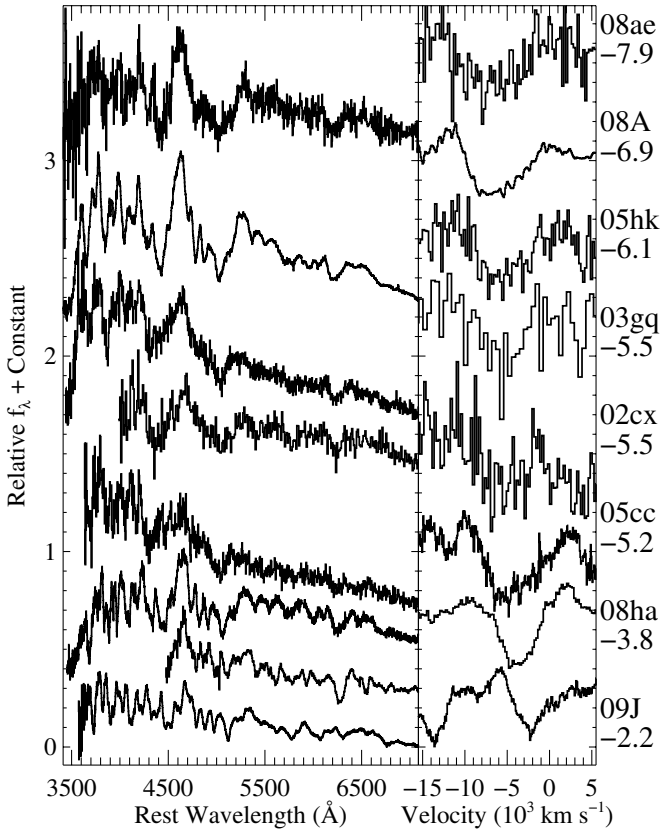


**Figure 18.** Near-maximum optical spectra of SNe 2008ae, 2008A, 2005hk, 2003gq, 2002cx, 2005cc, 2008ha, and 2009J from top to bottom. The respective phases relative to $V$ maximum are −2.4, −2.7, −5.9, −2.4, −3.2, −0.1, 3.2, and 0.2 days. The spectra have been ordered by their Si II λ6355 velocity. The right-hand panel displays the Si II λ6355 feature on a velocity scale. Narrow galactic features have been manually removed from some of the spectra. Each spectrum is labeled with the SN name and its Si II λ6355 velocity (in $10^{-3}$ km s$^{-1}$).

resolved, with all spectra having features attributed to C/O burning. Furthermore, the extreme SN 2008ha does not appear to be significantly different from the other members of the class, but rather there seems to be a spectral sequence for the objects defined primarily by ejecta velocity.

Using the method of Blondin et al. (2006) to measure photospheric velocities, we determine the temporal evolution of the Si II λ6355 feature for several members of the class. Figure 19 shows the results. Generally, the Si II velocity is relatively flat until a few days before $V$ maximum. At that time, the velocity decreases quickly, and around 10–15 days after $V$ maximum the velocity starts to decline more gradually. This behavior is slightly different from that of normal SNe Ia, where high-velocity features at early times can cause steep velocity declines at $t \lesssim -5$ days (e.g., Foley et al. 2012a), but is similar to the velocity evolution of some potential "Super-Chandrasekhar" SNe Ia (Scalzo et al. 2012), for which a thin, dense shell of material in the ejecta has been invoked to explain the low velocity gradients. For some SNe at times starting around 10–15 days after maximum brightness, the Si II feature begins to blend with other features, and the velocity is not a particularly reliable measurement.

Fitting the velocity data for $-6 < t < 15$ days, we measured the velocity gradients near maximum brightness. Unlike normal SNe Ia (Foley et al. 2011), there is no evidence for a correlation between the velocity gradient near maximum brightness and the velocity at maximum brightness. The individual velocity

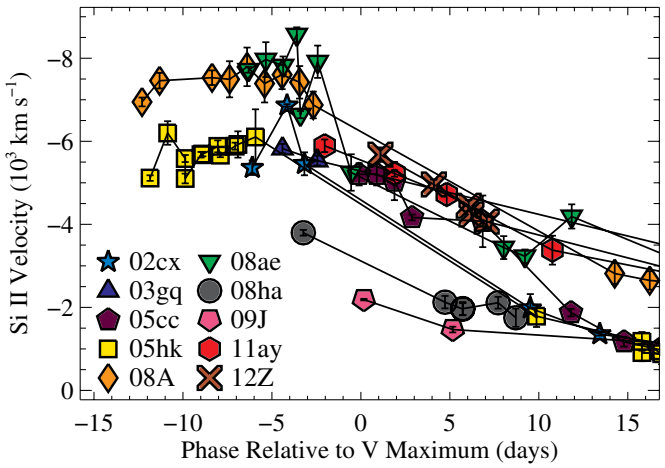


**Figure 19.** Si II λ6355 velocity as a function of time relative to $V$-band maximum brightness for SNe Iax.

(A color version of this figure is available in the online journal.)

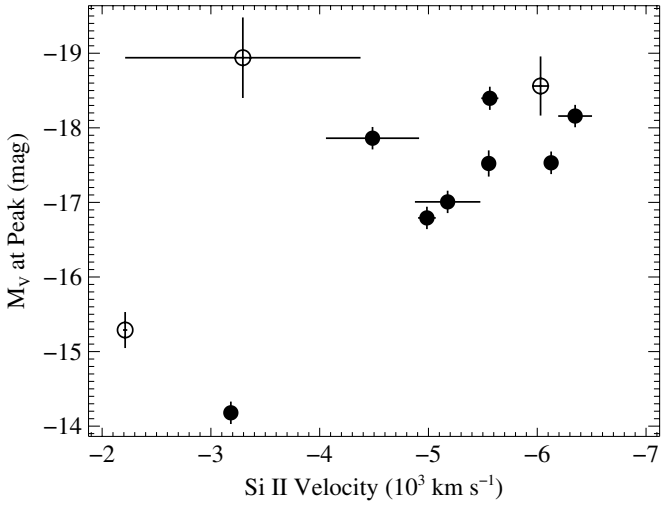


**Figure 20.** Si II λ6355 velocity vs. peak absolute $V$ magnitude for SNe Iax. SNe 2009J, 2009ku, and 2012Z, for which $M_V$ is estimated using the relations derived in Section 4.1, are represented by the empty circles, indicating their approximate values.

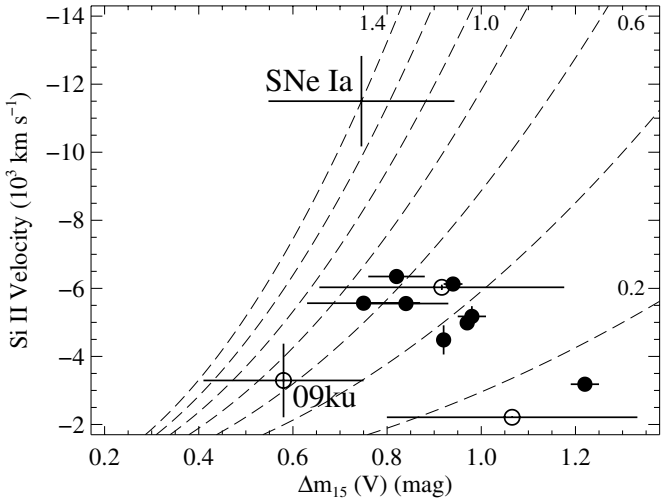


**Figure 21.** Light-curve shape vs. Si II λ6355 velocity for SNe Iax. SNe 2009J, 2009ku, and 2012Z, for which $\Delta m_{15}(V)$ is estimated using the relations derived in Section 4.1, are represented by the empty circles, indicating their approximate values. The average and standard deviation for normal SNe Ia are plotted as a single cross and labeled. The dashed lines represent lines of equal ejecta mass, ranging from 1.4 $M_\odot$ in the upper left to 0.2 $M_\odot$ in the lower right in steps of 0.2 $M_\odot$. The majority of SNe Iax cluster at ∼0.5 $M_\odot$.

gradients are all similar to the weighted mean of 250 km s$^{-1}$ day$^{-1}$, which is at the high end of velocity gradients for normal SNe Ia (Foley et al. 2011).

Using the data near maximum brightness, we simultaneously fit for the velocity at $V$ maximum when fitting for the velocity gradient. These range from −2210 (for SN 2009J) to −6350 km s$^{-1}$ (for SN 2008A). Near maximum, there is a larger spread in velocities than at later times. And although SNe with relatively high velocities at early times (like SNe 2008A and 2008ae) also have relatively high velocities at later times, some SNe with intermediate velocities at early times (like SNe 2002cx and 2005cc) at later times have velocities similar to those of SN 2008ha. Clearly, the velocity/density structure of the ejecta can be very different in these objects; nonetheless, we treat the maximum-light velocity as an indication of the photospheric velocity.

McClelland et al. (2010) suggested that there is a progression from extremely low-velocity, low-luminosity SNe like SN 2008ha through SNe more similar to SN 2002cx to normal SNe Ia with relatively high velocity and high luminosity. To do this, they measured the photospheric velocity at 10 days after $B$ maximum for SNe 2002cx, 2005hk, 2007qd, and 2008ha. (We note that we cannot reliably measure the time of maximum for SN 2007qd.) The velocity measurement was made by cross correlating the spectra. Although this method should produce reasonable results, we prefer our direct measurements to provide a reproducible result.

Narayan et al. (2011) countered the claims of McClelland et al. (2010) by presenting observations of SN 2009ku, which had low velocity and a high luminosity. Although it is clear that SN 2009ku was a low-velocity SN relative to SN 2002cx, its first spectrum was obtained 18 days after $B$ maximum, and we are unable to measure its Si II velocity at maximum brightness. However, based on spectral similarities, SN 2009ku likely had a velocity similar to that of SN 2008ha. For SN 2009ku, we assign a velocity intermediate between the first and third lowest-velocity SNe in our sample, SNe 2009J and 2005cc.

Figure 20 compares peak absolute magnitude and maximum-light velocity for the SNe Iax. Ignoring SN 2009ku, there is a slight trend where higher-velocity SNe are also more luminous. This trend may be stronger with additional data for SNe 2010ae and 2010el, which both have low velocities and low peak magnitudes (M. Stritzinger et al., in preparation; S. Valenti et al., in preparation).

Similar to Narayan et al. (2011), we also compare the maximum-light velocity to light-curve shape for SNe Iax in Figure 21. Again, ignoring SN 2009ku, there is a possible correlation, where higher-velocity SNe also have slower declining light curves. However, besides SNe 2008ha, 2009J, and 2009ku, SNe Iax occupy a relatively small portion of the parameter space.

In Figure 21, we also plot the average and standard deviation measurements for Si II velocity (Foley et al. 2011) and $\Delta m_{15}(V)$ (Hicken et al. 2009) for SNe Ia. As expected, normal SNe Ia have higher velocities than SNe Iax, but also typically have slightly slower decline rates. As was done by Narayan et al. (2011), we estimate the ejecta mass using analytical expressions of Arnett (1982), the decline rate in $V$ as a proxy for the bolometric rise time, and the ejecta velocity, and we scale the relations such

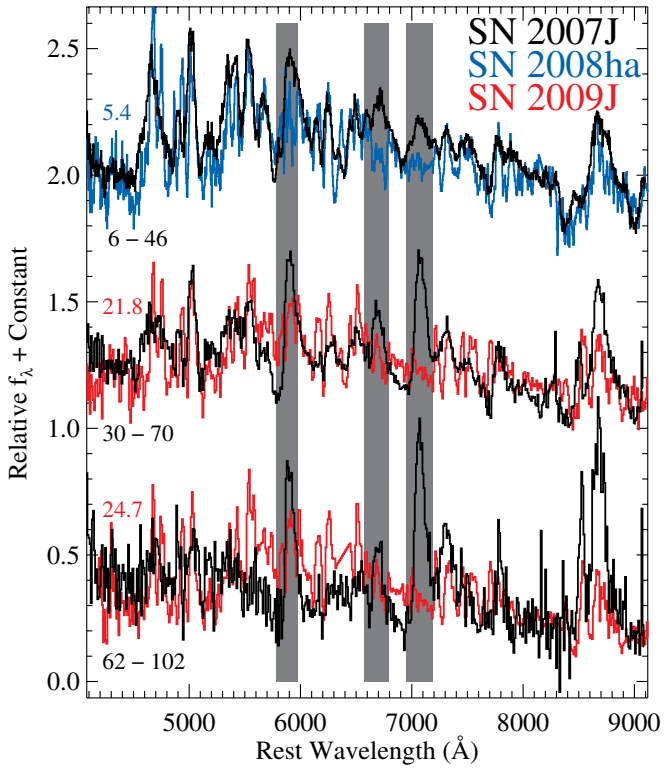


**Figure 22.** Spectral sequence of SN 2007J (black curves) compared to spectra of SNe 2008ha (blue) and 2009J (red). The phases (and phase ranges) are noted next to each spectrum. Wavelength regions corresponding to strong transitions of He I and ±5000 km s$^{-1}$ around those wavelengths are shaded gray.

(A color version of this figure is available in the online journal.)

that a normal SN Ia has an ejecta mass of 1.4 $M_\odot$. From this relation, we see that the majority of SNe Iax have ejecta masses of $\sim 0.5 \pm 0.2$ $M_\odot$, and SN 2008ha has an ejecta mass slightly below 0.2 $M_\odot$ (very similar to the 0.15 $M_\odot$ of ejecta estimated by Foley et al. 2009).

From these simple relations and scalings, it appears that the majority of SNe Iax have significantly less than a Chandrasekhar mass of ejecta. The luminosity gap between the majority of SNe Iax in our sample and SNe 2008ha/2009J may also be reflected in the apparent ejecta mass gap. Perhaps more low and intermediate-luminosity SNe Iax will produce a continuum of ejecta masses.

### 5.2. Presence and Frequency of Helium

As originally noted by Foley et al. (2009), SN 2007J is an SN Iax with strong He I features. These features developed over time, but are present even in our first spectrum of SN 2007J. Our spectral series of SN 2007J is displayed in Figure 22. The He I lines are relatively weak in the first SN 2007J spectrum, and it is not easy to distinguish this emission from normal SN Iax spectra (Filippenko et al. 2007a). However, the He I lines clearly exist when comparing the spectrum to that of SN 2008ha. In our next spectrum, corresponding to a phase of 30–70 days after maximum, the He I features become quite strong. In our final spectrum, at a phase of 62–102 days, the strongest He I line is the most prominent feature in the optical range. The spectrum of SN 2004cs presented in Figure 3 is at a phase of 42 days after $V$ maximum brightness, and also shows strong He I lines.

There is a phase where SN 2005E was spectroscopically similar to SN 2007J. Perets et al. (2010) presented three spectra of SN 2005E at phases of 9, 29, and 62 days relative to maximum brightness. The first and last spectra are clearly distinct from SN 2007J. Although a careful examination of the 29 day spectrum shows that it is different from those of SNe Iax, it could potentially be confused with an SN Iax, or alternatively, perhaps an SN Iax with helium can be confused with an SN 2005E-like object. The first and last SN 2007J spectra are separated by 60 days, so we expect that one of the SN 2007J spectra would resemble SN 2005E at another epoch if it were an SN 2005E-like object. Our SN 2004cs spectrum is at a phase of 42 days. This is intermediate between the second and third SN 2005E spectra. It is therefore possible that SN 2004cs is actually an SN 2005E-like object, but it is spectroscopically more similar to other SNe Iax than to SN 2005E.

We have identified two SNe Iax with He I lines in their spectra: SNe 2004cs and 2007J. No other SN Iax exhibits clear He emission. At a phase of ∼45 days after maximum brightness, the spectra of both SNe have strong He I lines. Several SNe Iax have spectra at phases similar to the SN 2007J spectra that show He features. We estimate that 9–14 SNe Iax have spectra that could rule out He features as strong as those of SNe 2004cs and 2007J. This provides a very rough estimate that ∼15% of SNe Iax show He features during the phases that SNe 2004cs and 2007J do.

As SN 2007J demonstrates, the frequency of He features is highly dependent on the phases of spectra obtained. It is also possible that many SNe Iax with He I lines are misclassified as SNe IIb and SNe Ib like SNe 2004cs and 2007J were (Rajala et al. 2005; Filippenko et al. 2007b). If that is the case, then the fraction would increase. Additionally, the strengths of He I features are highly dependent on density/mixing/temperature/ionization effects in addition to abundance. For instance, an outstanding question is how much helium exists in the ejecta of SNe Ic (e.g., Hachinger et al. 2012). Additionally, models of helium-shell (on top of a C/O WD) explosions tend to be asymmetric (e.g., Townsley et al. 2012), and one might expect that the helium distribution is asymmetric in an SN Iax explosion, resulting in viewing-angle-dependent spectral features.

Additional data, particularly spectral sequences covering a large phase range, as well as detailed modeling, will be necessary to determine the fraction of SNe Iax with He I features and ultimately the mass and distribution of helium in the ejecta.

### 5.3. Presence and Frequency of Carbon

The amount and distribution of carbon in SN Ia ejecta is a key discriminant between various explosion models (Gamezo et al. 2003). The presence of carbon also restricts certain progenitor systems. For instance, there should be little carbon in the ejecta of an electron-capture SN of an O-Mg-Ne WD. Depending on the temperature, it is possible to see C I, C II, and C III lines in an optical SN spectrum (Hatano et al. 1999), although C I has mostly weak optical lines blueward of ∼8000 Å.

Carbon lines have been detected in several normal SNe Ia, and ∼30% of high signal-to-noise ratio (S/N) SN Ia spectra obtained before maximum brightness show an indication of carbon absorption (Parrent et al. 2011; Thomas et al. 2011; Folatelli et al. 2012; Silverman & Filippenko 2012).

C II lines have been reported in SN 2008ha (Foley et al. 2010a), and possibly identified in SNe 2002cx (Parrent et al. 2011), 2005hk (Chornock et al. 2006), and 2007qd (McClelland et al. 2010). In Figure 23, we present these SNe along with several other SNe Iax that show some indication of C II.

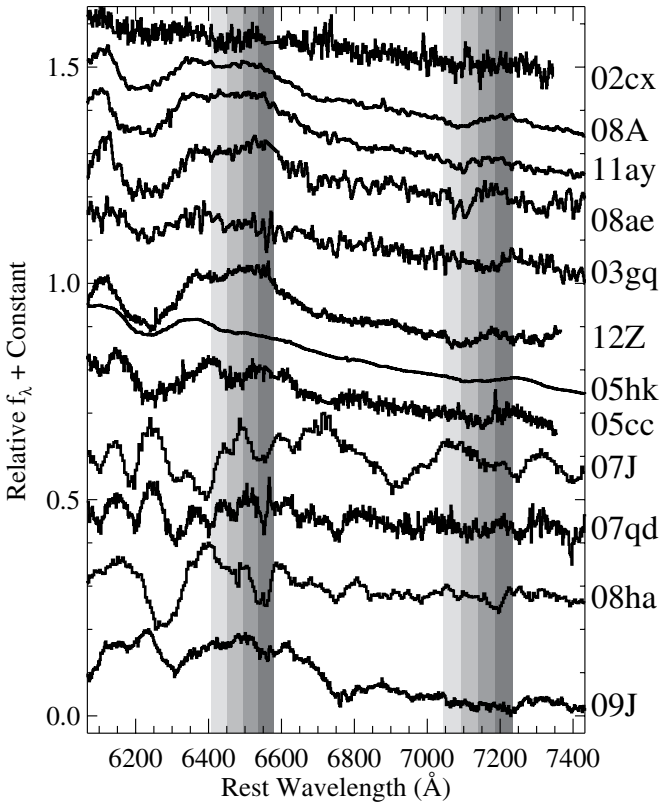


**Figure 23.** Optical spectra of SNe Iax showing the region covering the C II λ6580 and λ7234 lines. These spectra were chosen to best show the C II features. Each spectrum is labeled and ordered by approximate Si II velocity. The gray regions correspond to velocities for the C II lines spanning a width of 2000 km s$^{-1}$ each, and starting at 0, −2000, −4000, and −6000 km s$^{-1}$, respectively.

Specifically, SNe 2005cc, 2005hk, 2007qd, 2008A, 2008ae, 2008ha, 2009J, 2011ay, and 2012Z have clear detections of C II λ6580 and λ7234. SNe 2002cx and 2003gq also have features suggestive of C II. *Every* SN Iax with a spectrum before or around maximum light has some indication of carbon absorption.

The phase range for the spectra is from −9.9 to 1.1 days relative to $V$ maximum. Since some SNe Iax have very hot photospheres at early times, one might expect there to be relatively strong C III in those spectra. There is some indication that the early spectra of SNe 2005hk and 2012Z contain C III λ4647 and λ5696. Other spectra may also contain C III features, but spectral modeling may be required to clearly identify the features.

The high fraction (82–100%) of SNe Iax with carbon visible in their pre-maximum spectra is extremely interesting. There is no indication that our spectra have a significantly higher S/N than those used in previous studies to determine the fraction of SNe Ia with carbon in their spectra. With their lower velocities reducing the blending of C II λ6580 into the Si II λ6355 feature, it should be somewhat easier to detect C II in SNe Iax; however, only a small number (∼10%) of SNe Ia have velocities high enough to be affected by blending (Silverman & Filippenko 2012).

Clearly, there is a significant amount of carbon present in the ejecta of all SNe Iax. Using a modified model from Tanaka et al. (2011), Folatelli et al. (2012) determined the mass of carbon in SNe Ia by measuring the pseudo-equivalent width (pEW) of C II λ6580. The upper range of the measured pEWs is ∼4 Å at about 5 days before $B$ maximum and ∼1 Å near maximum. Several SNe Iax have stronger C II λ6580; for instance, SNe 2005cc and 2008ha have pEWs of 24 and 5 Å at phases of −3.2 and −0.1 days relative to $V$ maximum (∼−1.2 and 5.6 days relative to $B$ maximum), respectively. SN 2008ae, which has a relatively weak line, has a pEW of 3 Å at −5.3 (−0.2) days relative to $V$ ($B$) maximum. These values are all significantly higher than the observations of SNe Ia at similar phases. Although we do not produce additional models, it is clear that SNe Iax require significantly more carbon (by mass fraction) than do SNe Ia.

### 5.4. Late-time Spectra

SNe Iax have very different spectral sequences than SNe Ia (e.g., Jha et al. 2006; Sahu et al. 2008; Foley et al. 2010c). Specifically, we have not yet seen a truly nebular spectrum (one which is dominated by broad forbidden lines and lacks P-Cygni lines indicative of a photosphere) for any member of the class, despite observing these SNe >300 days after maximum brightness. All other known classes of SNe have nebular spectra at these phases.

In Figure 24, we present late-time spectra of the five SNe Iax with a well-determined time of maximum and spectra at $t >$ 150 days. We also include SN 2011ce, which has a late-time spectrum at a phase of about 383 days (see Section 2.24), and SN 2005P, which does not have a well-defined time of maximum, but whose spectrum is very similar to other late-time spectra of SNe Iax (Jha et al. 2006; Foley et al. 2010a). All spectra are similar, with the differences mainly being the observed velocities and the strengths of [Ca II], [Fe II], and [Ni II] features. None of these spectra are similar to those of SNe Ia, including low-luminosity SNe like SN 1991bg, or to SNe Ic. It is worth noting that SNe 2005hk, 2008A, 2011ay, and 2011ce were originally classified as members of this class from their first near-maximum spectra, and despite having relatively high ejecta velocities and peak absolute magnitudes similar to those of low-luminosity SNe Ia, their late-time spectra bear no resemblance to any SN Ia. Valenti et al. (2009) suggested that a late-time spectrum of SN 2005hk was similar to a late-time spectrum of the low-luminosity SN II 1997D (except lacking any hydrogen features). However, this similarity is likely because these objects cool through similar lines.

Despite generally looking similar, the SN Iax late-time spectra are still relatively distinct. The right-hand panel of Figure 24 shows the spectra in the region of the [Ca II]-[Fe II]-[Ni II] complex (around 7300 Å). SNe 2002cx, 2005hk, and 2011ce have low velocities for all features and very little emission in forbidden lines from Fe-group elements. SNe 2005P and 2008A have very similar spectra, with both having strong emission in forbidden lines from Fe-group elements and from [Ca II]. The spectrum of SN 2005P has slightly stronger [Fe II] compared to [Ni II] than SN 2008A. SN 2008ge has barely detectable [Ca II] emission and very strong [Ni II] emission. SN 2011ay is somewhat similar to SN 2008ge (lacking strong [Ca II] emission), but its phase is a bit earlier than that of the other SNe. Interestingly, the spectrum of SN 2008A looks extremely similar to that of SN 2008ge, except for additional [Ca II] emission. Moreover, the spectrum of SN 2005hk is very similar to those of SNe 2002cx and 2011ce, but it has exceptionally strong emission lines. Of the six SNe Iax with particularly late-time spectra (all SNe above except SN 2011ay), there are two equal-sized groups in velocity, with SNe 2002cx, 2005hk, and 2011ce all having similarly low velocities and SNe 2005P, 2008A, and 2008ge all having similarly high velocities.

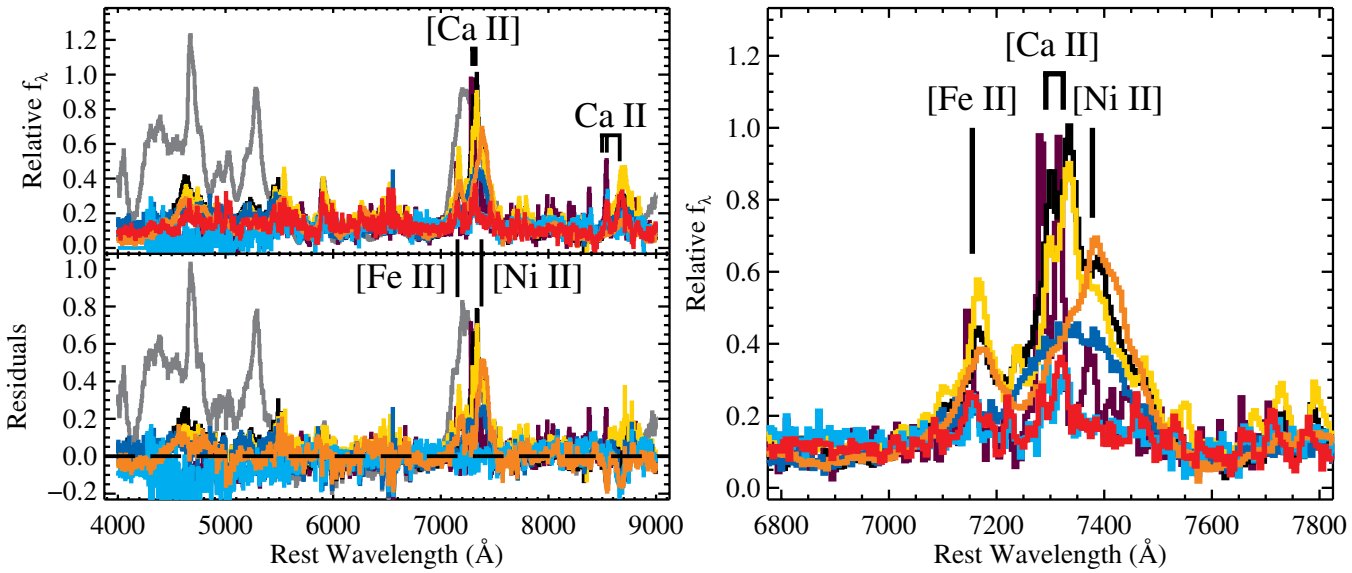


**Figure 24.** Late-time spectra of SNe Iax. The red, yellow, purple, black, gold, dark blue, and light-blue spectra correspond to SNe 2002cx, 2005P, 2005hk, 2008A, 2008ge, 2011ay, and 2011ce at phases of 227, an unknown phase, 224, 220, 225, 176, and 371 days, respectively. The gray spectrum is that of the SN 1991bg-like SN 1999by. The bottom-left panel displays the residual spectra relative to SN 2002cx. SNe 2005P, 2008A, 2008ge, and 2011ay have significant [Ni II] emission relative to SN 2002cx. The right panel shows the region near 7300 Å, and does not show the spectrum of SN 1999by.

(A color version of this figure is available in the online journal.)

In all cases where we can measure both [Fe II] and [Ni II], the [Ni II] emission is stronger than the [Fe II] emission. The opposite occurs in normal SNe Ia. By this phase, nearly all $^{56}$Ni has radioactively decayed. To have such a large [Ni II] to [Fe II] ratio, SNe Iax must produce significantly more stable Ni relative to radioactive Ni than SNe Ia, or significantly less stable Fe relative to radioactive Ni (and Co). Low-energy explosions of low-density/low-temperature material are predicted to produce such a trend (e.g., Travaglio et al. 2004).

The [Fe II] λ7155 line is the strongest [Fe II] feature in SN Iax spectra at late times. Normal SNe Ia tend to have stronger bluer Fe features such as [Fe II] λ5262 and [Fe III] λ4701, that are not (or perhaps weakly) detected in SNe Iax. The ejecta in SNe Iax must be relatively cold to produce these spectra (C. McCully et al., in preparation).

For SNe 2002cx, 2008A, and 2008ge, we are able to measure the width of the [Ca II] emission lines. The lines have full widths at half-maximum intensity (FWHMs) of 600, 1000, and 500 km s$^{-1}$, respectively. For SNe 2005hk and 2011ce, the FWHM is at or below the resolution of the spectra, 300 km s$^{-1}$. The measurement of SN 2008ge is particularly uncertain since the lines are weak. For SNe 2002cx, 2008A, 2008ge, and 2011ce, we measure FWHMs for [Fe II] λ7155 of 1200, 1200, 2900, and 500 km s$^{-1}$, respectively, with the line again being $\lesssim$300 km s$^{-1}$ for SN 2005hk. The [Fe II] lines are consistently broader than the [Ca II] lines, indicating that the Ca is *interior* to the Fe. Furthermore, the [Ca II] and [Fe II] FWHMs are not well correlated from object to object.

In addition to a diverse set of line widths, the nebular lines have diverse velocity shifts. If the ejecta are completely transparent (because we see P-Cygni features, the ejecta are not completely transparent, but we assume that they are mostly transparent), the line shifts should indicate any bulk offsets in the ejecta mapped by the lines relative to the center of mass of the ejecta. For SNe 2005hk, 2008A, and 2008ge, we are able to measure line shifts of [Fe II] λ7155, [Ca II] λλ7291, 7324, and [Ni II] λ7378. For SNe 2002cx and 2011ce, we could measure line shifts of the first two features. For SNe 2002cx, 2005hk, 2008A, 2008ge, and 2011ce we measure shifts of +60, +250, −560, −810, and +100 km s$^{-1}$ for [Fe II], and −220, −380, +450, +410, and +20 km s$^{-1}$ for [Ca II], respectively.

In all but one case, the [Fe II] and [Ca II] features have shifts in opposite directions, while in the three cases where [Ni II] was measured, the shift was in the same direction and had approximately the same magnitude as [Fe II]. The one outlier, SN 2011ce, has velocity shifts very close to zero. Interestingly, the two cases with blueshifted [Ca II] are SNe 2002cx and 2005hk, which have low-velocity late-time spectra, while SNe 2008A and 2008ge have redshifted [Ca II] and have high-velocity late-time spectra. SN 2011ce, which has a very small shift, also has low-velocities. The difference between the [Fe II] and [Ca II] velocities also roughly correlates with FWHM; SNe with narrower lines also have a smaller difference between [Fe II] and [Ca II] velocities.

Maeda et al. (2010) suggested that [Ni II] λ7178 comes primarily from the innermost ejecta of SNe Ia, tracing out electron-capture processes prevalent during the deflagration phase. The [Fe II] λ7155 line is supposed to track the high-density region directly outside the electron-capture zone and also is a tracer of the deflagration phase. Strong [Ca II] lines are not seen in nebular spectra of SNe Ia, but Ca should not be the result of supersonic burning. If Fe/Ni track the deflagration phase of C/O burning, then perhaps Ca tracks lower-energy or lower-density burning on the opposite side of the WD from the deflagration flame.

Although our current data are limited, it is clear that the velocity structure of SNe Iax is probably quite complex. Detailed spectral synthesis of various explosion models will be necessary to explain all behavior seen in the late-time spectra. Additionally, there is no clear correlation between late-time spectral features (velocities, line ratios, line strengths) and maximum-light properties (peak luminosity, light-curve shape, photospheric velocity). Models will have to simultaneously describe both the diversity of observables and their uncorrelated nature.

## 6. RATES

SNe Iax are the most common "peculiar" class of SNe. Thus far, they have been mostly ignored in SN rate calculations and quantities derived from those rates. Li et al. (2011) examined the prevalence of SNe Iax in the LOSS sample, finding that SNe Iax have a relative rate of $1.6^{+2.0}_{-1.2}$ and $5.7^{+5.5}_{-3.8}$ SNe Iax for every 100 SNe Ia in a magnitude-limited and volume-limited survey, respectively. However, this study was hampered by small numbers and the SNe used in the KAIT sample were all more luminous than $M = -16.7$ mag at peak. The KAIT study did not account for the low-luminosity SNe Iax, and thus, underestimated the true rate of SNe Iax. Meanwhile, Foley et al. (2009) estimated that SN 2008ha-like events could have a relative rate of ∼10 SNe Iax for every 100 SNe Ia. Simply combining the Li et al. (2011) estimate of the higher-luminosity SNe Iax and the Foley et al. (2009) estimate of SN 2008ha-like events results in an estimate of ∼17 SNe Iax for every 100 SNe Ia.

Thus far, only measurements of the fraction of SNe Ia being SNe Iax have been attempted. With our dataset, we do not have the proper information to derive a true SN rate. However, we can estimate the relative rate of SNe Iax to normal SNe Ia. We caution that our approach is limited by our heterogeneous dataset and assumptions built into the analysis. A significant uncertainty is the classification: several SNe Iax may exist without being properly classified. Since the discovery of SN 2002cx, 8 of the 21 recent members of the SN Iax class were originally misclassified, and one member was not classified for more than a year after discovery. Even within the BSNIP data release, which provides spectra for 11 members and classifications were performed recently, there was a single member (SN 2006hn) which was simply classified as a "SN Ia" (Silverman et al. 2012). Furthermore, BSNIP did not include SN 2007J because of its He lines. Nonetheless, Silverman et al. (2012) identified a previously unclassified SN as a member (SN 2002bp). Clearly, classification is difficult and some true members (even within the last 10 years) are not included in our current sample. As a result, our relative rate estimates are likely underestimates of the true relative rate.

With the above caveats, we wish to estimate the relative rate, or ratio, of SNe Iax to normal SNe Ia in a given volume. This is expressed as

$$r_{\rm Iax} = C_{\rm Iax} \frac{N_{\rm Iax}(\mu \leqslant \mu_{\rm max})}{N_{\rm Ia}(\mu \leqslant \mu_{\rm max})}, \quad (13)$$

where $\mu_{\rm max}$ is the maximum distance modulus for which one can detect SNe Iax in a survey, $N(\mu \leqslant \mu_{\rm max})$ is the number of SNe with a distance modulus less than $\mu_{\rm max}$, and $C_{\rm Iax}$ is a correction factor to account for various observational effects. For a given survey, we have

$$\mu_{\rm max} = m_{\rm lim} - M, \quad (14)$$

where $m_{\rm lim}$ is the limiting magnitude of the survey and $M$ is that absolute magnitude of an SN Iax. For this study, we will focus on $R_{\rm Iax} = 100 r_{\rm Iax}$, the number of SNe Iax expected for every 100 SNe Ia in a given volume.

For our calculation, we will focus on SNe discovered with nearby surveys. We therefore exclude from our analysis SNe 2007ie, 2007qd, and 2009ku, which were discovered (exclusively) by the SDSS-II SN Survey and PS1. For nearby surveys, the typical limit is $m_{\rm lim} \approx 18.5$ mag. Nearby surveys have varying cadences, but are typically 5–15 days, and are usually conducted in a band similar to $R$. We therefore define

$$M = M_{R,\rm peak} + A_{R,\rm MW} + \Delta m_{15}(R). \quad (15)$$

We adjust the peak absolute magnitude by $\Delta m_{15}$ to guarantee that the SN will be detected in at least two images. We also correct for Milky Way extinction since dust obscuration will affect a survey's ability to discover SNe.

Although we do not know the SN Iax luminosity function, we have measured the peak absolute magnitude and decline rate for several members. From these measurements, we determined a set of $\mu_{\rm max}$, which are the maximum distance moduli at which we would detect each of those SNe.

The least luminous SN in the class is SN 2008ha, which is at $\mu = 31.65$ mag. The nominal scheme outlined above yields $\mu_{\rm lim} = 31.60$ mag for SN 2008ha. Having $\mu_{\rm lim} < \mu$ is likely the result of faster cadences for very nearby galaxies; thus, we choose $\mu_{\rm lim} = 31.65$ mag for SN 2008ha. If there are no SNe significantly fainter than SN 2008ha, then we expect the sample within this volume to be reasonably complete, resulting in a relatively unbiased first look at the relative rate.

In the 10 years following the discovery of SN 2002cx, there have been 22 normal SNe Ia and 4 SNe Iax (SNe 2008ge, 2008ha, 2010ae, and 2010el) discovered within $\mu_{\rm lim} = 31.65$ mag (from the Asiago SN catalog; Barbon et al. 1989). Unless there are significantly more SNe Iax with luminosities less than SN 2008ha, this sample should be relatively complete for monitored galaxies (with the exception of misclassification, cadence, seasons, and weather). Using Poisson statistics within this volume, the uncorrected ($C_{\rm Iax} = 1$) relative rate is $R_{\rm Iax} = 18^{+12}_{-9}$. SNe 2010ae and 2010el have peak luminosities similar to that of SN 2008ha (M. Stritzinger et al., in preparation; S. Valenti et al., in preparation), while SN 2008ge is much more luminous than SN 2008ha (Foley et al. 2010c). If SNe 2008ha, 2010ae, or 2010el had exploded when they were in close proximity to the Sun, then we would not have detected the SNe, while any SN Ia within that distance could have been discovered more than six months after explosion. Because of that and other factors (host-galaxy dust reddening, weather, etc.), we perform the same analysis, but with $C_{\rm Iax} = 2$ for SNe 2008ha, 2010ae, and 2010el, and $C_{\rm Iax} = 1$ for SN 2008ge. This then gives a corrected relative rate of $R_{\rm Iax} = 30^{+21}_{-15}$.

We can also place a relatively robust lower limit on the relative rate using all 19 members found by nearby surveys since the discovery of SN 2002cx. Of the members of the class with good $R$-band light curves, SN 2008A is the most luminous. Within the volume defined by its $\mu_{\rm lim}$, there have been 573 spectroscopically normal SNe Ia as derived from the Asiago catalog with distances cross-matched to NED. Within this volume, all SNe Ia (with the exception of those with extreme dust extinction) should be detectable for several months. We exclude the peculiar SNe 2006bt (Foley et al. 2010b) and 2009dc (e.g., Yamanaka et al. 2009; Tanaka et al. 2010; Silverman et al. 2011b), as well as SNe with redshifts only derived from SN features (since these SNe could be potential SNe Iax). Without any corrections for luminosity or effects related to the surveys, we find $R_{\rm Iax} = 3.3^{+0.8}_{-0.7}$. This method is similar to what was done by Li et al. (2011), where only the most luminous SNe Iax were included in the rate calculation. Unsurprisingly, our derived fraction is similar to the fraction from Li et al. (2011).

We now perform a more thorough treatment with the 19 members found by nearby surveys since the discovery of SN 2002cx, including SN 2002cx. For this, we assume a

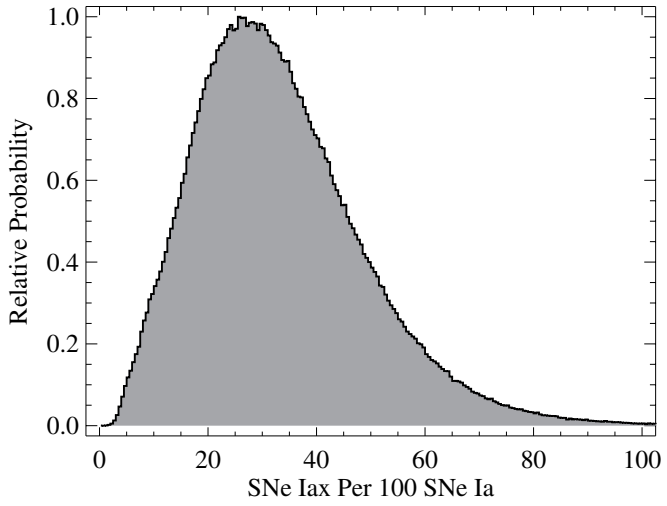


**Figure 25.** Probability density function for the SN Iax rate relative to the SN Ia rate.

luminosity function that has equal probability of an SN having the luminosity of any of the 6 SNe with measured $M_{R,\mathrm{peak}}$ and another, SN 2009J, which has a first measurement that appears to be at peak. Our sample, which is composed of SNe discovered by magnitude-limited surveys, almost certainly underrepresents the fraction of low-luminosity SNe Iax, which should result in an underestimated relative rate.

The flat luminosity function produces seven nested volumes. If a member lies within the first volume (defined by SN 2008ha), then it could have a luminosity similar to any of the SNe defining the luminosity function. We therefore assign it a fractional membership to each volume (in this case, 1/7th of an SN per volume). For each SN without a well-defined peak magnitude, we attempt to determine limits on its absolute magnitude from photometry reported in the literature and its distance modulus. We use this information to place further constraints on the fraction of SNe in each volume. For example, SN 2008ge, which was discovered within the volume defined by SN 2008ha, is much more luminous ($M_{V,\mathrm{peak}} = -17.60$ mag) than SN 2008ha. It therefore does not contribute to the rate of "SN 2008ha-like" SNe. SNe 2010ae and 2010el have $M_{V,\mathrm{peak}} \approx -15.0$ and $-14.7$ mag, respectively (M. Stritzinger et al., in preparation; S. Valenti et al., in preparation). These magnitudes were estimated from $B$ and $r$ light curves and converted using the relations outlined in Section 4. However, these relations may not adequately describe SNe similar to SN 2008ha. For instance, from the $B$-band light curve, SN 2010ae has $M_{B,\mathrm{peak}} \approx -13.9$ mag, only 0.2 mag brighter than SN 2008ha, but after converting the estimated $M_{V,\mathrm{peak}}$ for SN 2010ae is 0.8 mag brighter than SN 2008ha. Because of the potential errors in the peak-magnitude estimates along with uncertainties in reddening and distance moduli, we include SNe 2010ae and 2010el as having equal chance of being in the first two volumes.

For the reasons listed above as well as possible misclassifications for fainter SNe, we assume $C_{\mathrm{Iax}} = 2$. However, if $C_{\mathrm{Iax}} = 2$ for the three closest volumes and $C_{\mathrm{Iax}} = 1$ for the rest or if $C_{\mathrm{Iax}} = 1.5$ for all volumes, then the relative rate decreases by 13% and 8%, respectively. The corrected relative rate (with $C_{\mathrm{Iax}} = 2$) is $R_{\mathrm{Iax}} = 31^{+17}_{-13}$; however, as seen in Figure 25, the probability distribution function is slightly skewed with there being 3% and 14% chances that the relative rate is $R_{\mathrm{Iax}} < 10$ and $R_{\mathrm{Iax}} > 50$, respectively.

Our final, best relative rate of $R_{\mathrm{Iax}} = 31^{+17}_{-13}$ is very similar to what was found using only the most nearby SNe: $R_{\mathrm{Iax}} = 30^{+21}_{-15}$. This agreement provides an additional level of confidence for our values. Both values are marginally consistent with the combined Foley et al. (2009) and Li et al. (2011) rates of $R_{\mathrm{Iax}} \approx 17$.

We can now estimate the amount of Fe generated by SN Iax explosions relative to that of SNe Ia. Our estimate relies on the assumption that the luminosity of SNe Iax are powered primarily by $^{56}$Ni and its radioactive products; if they are powered by other radioactive elements, then the scalings assumed here would not apply. The other assumption is that the ratio of $^{56}$Ni to stable $^{54}$Fe is the same (on average) for SNe Ia and SNe Iax. For our estimate, we use the $^{56}$Ni masses estimated by Foley et al. (2009) for SN 2008ha ($(3.0 \pm 0.9) \times 10^{-3}\ M_{\odot}$) and Phillips et al. (2007) for SN 2005hk ($0.2 \pm 0.05\ M_{\odot}$). Since SN 2005hk has well-sampled UV through NIR light curves, its $^{56}$Ni mass is relatively robust. We then estimate the $^{56}$Ni mass for all other SNe in our luminosity-function sample by scaling the $^{56}$Ni mass of SN 2005hk by the ratio of their peak $R$-band luminosity. These estimates will be somewhat incorrect (by a factor of at most two) if the rise times of those SNe differ significantly from that of SN 2005hk or if they have significantly different colors. For our sample, the $^{56}$Ni mass ranges from 0.003 to 0.27 $M_{\odot}$.

To determine the amount of $^{56}$Ni produced by SNe Ia, we use the Stritzinger et al. (2006) sample of SNe Ia. This sample, which may be biased slightly, consists primarily of nearby SNe, and therefore should be similar to a volume-limited sample. From this sample, we exclude the peculiar SN 2000cx (Li et al. 2001a). Li et al. (2011) found that 74.0%, 10.0%, and 16.1% of SNe Ia in a volume-limited sample are "normal," similar to SN 1991T and SN 1991bg, respectively. The Stritzinger et al. (2006) sample has similar percentages of 67%, 20%, and 13%, respectively, but slightly over-represents and under-represents SNe similar to SNe 1991T and 1991bg, respectively.

The SNe Ia in the Stritzinger et al. (2006) sample produce on average, $0.24 \pm 0.02\ M_{\odot}$ of $^{56}$Ni. The median $^{56}$Ni in the sample is $0.66 \pm 0.18\ M_{\odot}$. When comparing the SN Iax sample to SNe Ia, we must assume that the ratio of $^{56}$Ni generated in the explosion to the total amount of Fe produced (both stable Fe in the explosion and that which decays from $^{56}$Ni) is the same for both classes. However, there is evidence from the late-time spectra that this is not the case (Section 5.4).

Using the rate calculation performed above and the average $^{56}$Ni value for SNe Ia, but weighting each luminosity bin and the SN Ia population by the appropriate $^{56}$Ni mass, we determine that SNe Iax produce $0.052^{+0.016}_{-0.014}\ M_{\odot}$ of Fe for every $M_{\odot}$ of Fe produced by SNe Ia. Using the median $^{56}$Ni value for SNe Ia, we find that SNe Iax produce $0.019^{+0.010}_{-0.006}\ M_{\odot}$ of Fe for every $M_{\odot}$ of Fe produced by SNe Ia. The values based on the different assumptions about the SN Ia $^{56}$Ni production differ by $<2\ \sigma$.

Because of the low $^{56}$Ni yield of SN 2008ha-like objects, this estimate is relatively unaffected by their inclusion in the rate calculation. Of course, the estimate of relative Fe production is fairly uncertain. Besides the caveats related to the rates above and the normalization of $^{56}$Ni mass, there is also the possibility that SNe Iax produce significantly less stable Fe for the amount of $^{56}$Ni produced (see Section 5.4). More importantly, we only estimate the Fe production for $z = 0$. The SN Ia rate rises with redshift to at least $z \approx 1$ (Graur et al. 2011), but since SNe Iax are associated with star-forming galaxies, one would expect the ratio of SNe Iax to SNe Ia (although perhaps not the Fe

generation) to increase with redshift. However, we estimate that at $z = 0$, SNe Ia produce about 0.036 $M_\odot$ of Fe for every $M_\odot$ of Fe produced by SNe Ia.

## 7. IMPLICATIONS FOR THE PROGENITOR SYSTEM

In the preceding sections, we have identified a number of observational characteristics for the SN Iax class. Here, we summarize these observations and explore their implications for a progenitor system. Specifically, we have noted the following.

1. SNe Iax have spectral and photometric properties that are similar to those of SNe Ia, but are distinct in several ways.
2. The class has a continuum in both luminosity and ejecta velocity. SN 2008ha, although on the extreme end of the spectrum for both quantities, is an extension of this continuum and not an outlier.
3. There is a large range of peak luminosity ($-14.2 \geqslant M_{V,\mathrm{peak}} \gtrsim -18.4$ mag) and velocity at maximum brightness ($2000 \lesssim |v| \lesssim 8000$ km s$^{-1}$). These ranges indicate a large range in explosion energies, ejecta masses, and $^{56}$Ni masses.
4. SN Iax light-curve shape and luminosity are correlated (a WLR), similar to that of SNe Ia, but with larger scatter.
5. The color curves of SNe Iax are similar in shape, but a simple reddening correction cannot reduce the scatter in all colors at once. This indicates a more complicated spectral energy distribution at intermediate phases for SNe Iax than for SNe Ia. The lack of host-galaxy reddening corrections probably contributes to some of the additional scatter in the WLR.
6. There is a slight correlation between peak luminosity and ejecta velocity.
7. Using basic assumptions, we estimate a wide range of ejecta masses for SNe Iax (from $\sim$0.2 to possibly $\sim$1.4 $M_\odot$), but most SNe Iax have $\sim$0.5 $M_\odot$ of ejecta.
8. All SNe Iax with maximum-light spectra, including SN 2008ha, show clear signs of C/O burning in their maximum-light spectra.
9. There is significant mixing of the ejecta with both IMEs and Fe-group elements in all layers.
10. There are two SNe Iax that show helium lines in their spectra. Because of radiative-transfer effects, viewing-angle dependencies, and other effects, perhaps all SNe Iax have significant amounts of helium in their ejecta. Since helium should not be synthesized in the explosion, there must be helium somewhere in the progenitor systems of these two events.
11. Every SN Iax with a pre-maximum spectrum has some indication of carbon in the spectrum, with 82% having clear absorption. SNe Ia, on the other hand, show carbon in only 30% of SNe Ia with pre-maximum spectra. By mass fraction, SNe Iax should have significantly more carbon than SNe Ia.
12. Late-time spectra of SNe Iax are very different from those of SNe Ia, with no truly nebular spectrum of an SN Iax yet being observed.
13. In detail, the late-time spectra of SNe Iax differ significantly from object to object. Specifically, the strengths of various forbidden lines and the velocities of both the permitted and forbidden lines vary significantly between different SNe.
14. Unlike SNe 2002cx and 2005hk (Jha et al. 2006; Sahu et al. 2008), not all SNe Iax have exclusively low-velocity features in their late-time spectra. Some have [Fe II] FWHMs of $\sim$3000 km s$^{-1}$.
15. All SNe Iax for which we have late-time spectra have calcium interior to iron. This is the opposite of what is seen in SNe Ia.
16. In the late-time spectra, the [Ni II] $\lambda$7378 feature is typically stronger than the [Fe II] $\lambda$7155 feature. This indicates that SNe Iax either produce much more stable Ni or much less stable Fe than SNe Ia. This is a prediction of a low-energy, low-density explosion (e.g., Travaglio et al. 2004).
17. The large-velocity line shifts of forbidden nebular lines suggest that the explosion was asymmetric.
18. The late-time spectra can be divided into distinct groups having lower and higher velocities. The lower-velocity group tends to have blueshifted Ca and redshifted Fe, as determined by velocity shifts in forbidden lines, along our line of site. The opposite is true for the higher-velocity group. There is no evidence for a correlation between the line shifts (or equivalently velocities at late times) and maximum-light observables.
19. Because of their large range in luminosity, SNe Iax have been undercounted in previous rate estimates. Through a basic analysis, we find that in a given volume, for every 100 SNe Ia there should be $31^{+17}_{-13}$ SNe Iax, although even this number is likely a low estimate.
20. Although SNe Iax are relatively numerous, a large fraction of the population consists of low-luminosity events which likely produce little Fe. We estimate that SNe Iax produce $\sim$0.036 $M_\odot$ of Fe for every $M_\odot$ of Fe produced by SNe Ia.

In addition to these findings, others have noted the following.

21. A lack of a second maximum in the NIR (Li et al. 2003).
22. A host-galaxy morphology distribution highly skewed to late-type galaxies (Foley et al. 2009; Valenti et al. 2009).
23. SN 2005hk had very low polarization near maximum brightness, indicating nearly spherical outer ejecta (Chornock et al. 2006; Maund et al. 2010).
24. A lack of X-ray detections with 5 SNe Ia having $3\sigma$ luminosity limits below $9 \times 10^{39}$ erg s$^{-1}$ and 3 (SNe 2008ge, 2008ha, and 2010ae) below $2.7 \times 10^{39}$ erg s$^{-1}$ (Russell & Immler 2012). These limits are below most, but not all, detections and limits for stripped-envelope core-collapse SNe at early times (Perna et al. 2008).
25. The host galaxy of SN 2008ge is an S0 galaxy with no signs of star formation to deep limits. Additionally, pre-explosion *HST* images indicate that there are no massive stars at or near the SN site to deep limits.

It is remarkable that a long list of common properties applies to a large sample given the small number of observational criteria used to define the class. This is a clear indication that the SNe classified as Type Iax are physically similar, representing a physical class and not simply an observational class.

The above list of properties for SNe Iax provides robust tests for progenitor/explosion models. Below, we examine the various properties to constrain the set of possible scenarios. During this analysis, we assume that all members identified as SNe Iax share a common progenitor system and explosion mechanism, although the details of that explosion may vary. However, it is possible that we have incorrectly grouped physically distinct SNe into this single class. There may also be multiple progenitor paths to create an SN Iax. Because of the relatively small data, we do not attempt to further subdivide the class.

First, there are many reasons to believe that the progenitor star was a WD. The progenitor of SN 2008ge was most likely a WD with no indication of massive stars near the SN site

and strict limits on star formation in its host galaxy. More broadly, the estimated ejecta masses are all equal to or below a Chandrasekhar mass. If the progenitors were massive stars, then one would expect that at least occasionally this limit would be exceeded. Additionally, SNe Iax over the full luminosity range shows clear signs of C/O burning, which is not expected in a core-collapse SN.

However, complete thermonuclear burning of a WD cannot reproduce the velocities observed and ejecta masses inferred. Roughly, a 0.5 $M_{\odot}$ WD will be completely unbound and have ejecta velocities >2000 (6000) km s$^{-1}$ for pure helium to nickel or pure carbon to nickel burning efficiencies of >4% and 7% (15% and 24%), respectively. That is, if 10% of the carbon in a 0.5 $M_{\odot}$ WD is burned to $^{56}$Ni, then the star will be unbound and the ejecta velocity will be larger than 6000 km s$^{-1}$. This implies incredibly inefficient burning, either by traditional burning of a small percentage of the WD mass or by a more exotic, less efficient nuclear burning through the entire star.

Furthermore, SNe 2004cs and 2007J have helium in their spectra, and therefore there must be helium in the progenitor system. There is no hydrogen in any spectra, suggesting that hydrogen is most likely absent in the progenitor system. This indicates that either a He WD or a nondegenerate He star is in the system. The ejecta mass from a He WD explosion should not exceed ∼0.4 $M_{\odot}$, making it an unlikely progenitor star. It is possible that a He WD could be the binary companion of the primary star, but then one would expect there to be many SNe Iax in early-type host galaxies. Having any He WD in the progenitor system is unlikely, and instead, a He-burning-star companion to a C/O WD is the most likely progenitor system.

Tutukov & Yungelson (1996) predicted that C/O-He-burning-star progenitor systems could have a rate similar to the Galactic SN Ia rate, but would not explain the SNe Ia in older stellar populations. Performing a detailed population-synthesis analysis, Ruiter et al. (2011) found that 13% of sub-Chandrasekhar mass thermonuclear SNe could come from a C/O WD-He star channel. Assuming that this channel produces SNe Iax and other channels produce SNe Ia, the population-synthesis rate is roughly consistent with our measured rate. This channel has a relatively short delay time of ∼500 Myr, which should restrict the host-galaxy population to mostly spiral galaxies, but could include some SNe in S0 galaxies (like SN 2008ge).

A single system has been identified as a C/O WD with a He-burning-star companion for which mass transfer will begin before the end of the He-burning phase (Geier et al. 2012; Vennes et al. 2012). This system should be able to transfer mass for ∼50 Myr at a rate of $\sim 10^{-9}$ $M_{\odot}$ year$^{-1}$ for a potential total mass of ∼0.05 $M_{\odot}$ of material.

At certain accretion rates, He mass transfer to a C/O WD can occur without periodic He flashes, resulting in a massive He shell. In this scenario (e.g., Iben & Tutukov 1991; Tutukov & Yungelson 1996), after the WD acquires a significant He layer, the He layer can detonate, possibly causing a thermonuclear explosion within the C/O layer (Livne 1990; Woosley & Weaver 1994; Livne & Arnett 1995); this is sometimes called an "edge-lit" explosion.

For C/O WDs with large He layers, most theoretical studies have focused on "double-detonation" models where the He layer detonates (e.g., Nomoto 1982; Sim et al. 2012; Townsley et al. 2012), which in turn causes a detonation with the C/O layer (e.g., Nomoto 1982; Fink et al. 2010; Sim et al. 2012). Although there is still some discussion about the details of these explosions, the consensus is that it is difficult to reproduce the full diversity of SNe Iax with this mechanism.

In addition to "double-detonation" models, it is possible to detonate the He layer without causing the rest of the star to explode. This ".Ia" model (Bildsten et al. 2007; Shen et al. 2010) shares many characteristics with SNe Iax. Shen et al. (2010) and Waldman et al. (2011) examine the details of this model for high-mass and low-mass C/O cores, respectively. These models roughly match the characteristics and the diversity of SNe Iax, but it is unclear if they reproduce the explosions in detail. In particular, it is difficult to produce IMEs in these explosions, particularly for those on top of a high-mass core. These explosions also have low luminosity, so it appears difficult to reproduce SN 2002cx and more luminous SNe using this model. Foley et al. (2009) examine how these models match observations in detail.

The single C/O WD/He-burning-star system should produce a helium layer that is ∼0.05 $M_{\odot}$ to perhaps 0.3 $M_{\odot}$ (Iben & Tutukov 1991). Although this mass may not be enough to account for all of the ejecta in SNe Iax, it should be massive enough to detonate, perhaps triggering a double-detonation on a sub-Chandrasekhar mass SN (Fink et al. 2010). Sim et al. (2012) examined double-detonation models for relatively low-mass sub-Chandrasekhar C/O WDs with ∼0.2 $M_{\odot}$ He shells. The resulting observables were somewhat consistent with some SNe Iax ($\Delta m_{15} \approx 2$ mag, $t_{\rm rise} \approx 10$ days, low luminosity, low velocity).

Woosley & Kasen (2011) explored possible sub-Chandrasekhar-mass explosion models, some of which had a He-layer detonation or deflagration. The models, which only burned the He layer, and are somewhat similar to the.Ia model of Bildsten et al. (2007), roughly match the observables of SNe Iax. However, these models should be exclusively low luminosity, low ejecta mass, and contain a significant amount of unburned He. These models have difficulty reproducing all of the characteristics of all SNe Iax and the full ranges of those characteristics, particularly the luminosity range. Because of non-thermal effects that are not fully modeled in the radiative transfer, it is unclear if He lines should be strong in the spectra of these events.

A promising model for SNe Iax is a failed deflagration of a C/O WD. In this model, a burning flame within the WD rises to the surface, expelling ∼0.2–0.4 $M_{\odot}$ of material, some of which is the ash from the burning. In this model, the full WD is not consumed by the nuclear burning, and the entire star is not disrupted. This model was first proposed by Foley et al. (2009) as a possible explanation for SNe Iax. Model luminosity, ejecta mass, and velocity are all consistent with SNe Iax (Jordan et al. 2012; Kromer et al. 2012). It is unclear if this scenario requires a thick He shell or if the He shell potentially changes the explosion properties, but it is possible that a He-shell explosion could trigger a failed deflagration within the C/O core. Stable helium accretion occurs at a higher rate than stable hydrogen accretion, and thus the WD density and temperature structure are different for the two scenarios. These differences may be important in understanding the nature of SN Iax explosions. Alternatively, since a He layer appears to be important in creating SNe Iax, one might assume that an initial He-layer explosion is necessary to produce SNe Iax. Detailed modeling of nucleosynthetic products and the resulting light curves and spectra are still required, but one expects products similar to those of a normal SN Ia with perhaps additional unburned

material. This model continues to be the most promising yet proposed.

Assuming that all SNe Iax come from the same progenitor system and have the same explosion mechanism, the most promising model for SNe Iax is the deflagration of a C/O WD, either triggered by an explosion in an outer He layer or under conditions only met when stable He accretion occurs. The C/O WD would have a He-star binary companion. A scenario very similar to this was first proposed by Iben & Tutukov (1991). At least some of the time, and perhaps in all cases, the deflagration fails to unbind the WD, leaving a stellar remnant that may be observationally distinct from most WDs. Specifically, given the large velocity shifts for nebular lines in the late-time spectra of SNe Iax, one might expect a large kick for the remnant. Similarly, the energy injection and chemical enrichment may produce a puffed-up WD with peculiar abundances (Jordan et al. 2012; Kromer et al. 2012). This remnant may have particular observational signatures.

Perets et al. (2010) and Sullivan et al. (2011) both suggested similar explosion mechanisms, particularly He detonations on C/O WDs, for SN 2005E and PTF 09dav, respectively. These SNe share many characteristics with SNe Iax, including luminosity, velocity, and ejecta mass. However, both SN 2005E and PTF 09dav appear to come from old stellar populations (although PTF 09dav had hydrogen in its late-time spectrum; Kasliwal et al. 2012). In particular, the host-galaxy morphology distribution of SNe similar to SN 2005E is highly skewed to early-type galaxies (Perets et al. 2010), the opposite of SNe Iax. SN 2005E and similar objects all show relatively strong He at early times, again indicating He in the progenitor system. Perhaps SNe Iax are created in the above scenario and SN 2005E was produced in a very similar scenario, except with a He WD companion instead of a nondegenerate He star. This difference would account for the difference in stellar populations, and the accretion of degenerate and nondegenerate He could change the stable accretion rates and/or nucleosynthesis enough to create noticeably different events.

## 8. CONCLUSIONS

We have described in detail the observational properties of the Type Iax class of SNe. An SN is a member of this class if it has four observational properties, three of which can be determined from a single maximum-light spectrum: (1) no evidence of hydrogen in any spectrum, (2) relatively low ejecta velocity near maximum brightness ($|v| \lesssim 8000$ km s$^{-1}$), (3) an absolute magnitude that is low relative to an SN Ia with the same light-curve shape, and (4) spectra that are similar to SN 2002cx at similar epochs. Using these criteria, we have identified 25 members of this class. We presented optical photometry and spectroscopy for various members of this class.

SNe Iax represent a distinct stellar endpoint from SNe Ia and other common SNe. The class has a large range of luminosities, ejecta velocities, and inferred ejecta masses. Although there are clear signs of C/O burning in their ejecta, some SNe Iax also have He I lines in their spectra. As a possible progenitor system, a C/O WD that accretes from a nondegenerate He star and undergoes a (sometimes partial) deflagration matches the SN observables. The lifetimes of such systems are consistent with the SN Iax host-galaxy morphology distribution. Similarly, the rates of explosions from these systems roughly match the measured rates of $31^{+17}_{-13}$ SNe Iax for every 100 SNe Ia. This is perhaps a simplified view of the real physical picture, and future observations will test this model.

Additional studies of the details of the properties of SNe Iax should improve our knowledge of both this class of SN as well as providing insight into normal SNe Ia. For instance, if C/O WD-He-star systems exclusively produce SNe Iax, then we can rule out these systems as normal SN Ia progenitors.

SNe Iax are relatively common (about a third as common as SNe Ia at $z = 0$), and deep transient surveys of the local universe should discover a significant number. LSST is expected to discover $\sim 10^6$ SNe over its lifetime. Even taking the conservative, magnitude-limited rate for SNe Iax, LSST should discover more than $10^4$ SNe Iax, similar to the number of SNe Ia discovered to this day. Additionally, because of their frequency, we will continue to discover many in the very local universe ($D \lesssim 20$ Mpc), allowing detailed studies of individual objects and their stellar environments. The combination of thorough studies of local events and an upcoming large sample will undoubtedly improve our understanding of this recently discovered class of stellar explosion.

R.J.F. is supported by a Clay Fellowship. Supernova research at Harvard is supported by NSF grant AST–1211196. A.V.F.'s supernova group at U.C. Berkeley is supported by Gary & Cynthia Bengier, the Richard & Rhoda Goldman Fund, the Christopher R. Redlich Fund, the TABASGO Foundation, and NSF grants AST-0908886 and AST-1211916. KAIT and its ongoing operation were made possible by donations from Sun Microsystems, Inc., the Hewlett-Packard Company, AutoScope Corporation, Lick Observatory, the NSF, the University of California, the Sylvia & Jim Katzman Foundation, and the TABASGO Foundation. CSP material is based upon work supported by the NSF under grants AST-0306969, AST-0607438, and AST-1008343. M.S. acknowledges generous support provided by the Danish Agency for Science and Technology and Innovation through a Sapere Aude Level 2 grant. J.A., M.H., and G.P. acknowledge support provided by the Millennium Center for Supernova Science through grant P10-064-F (funded by "Programa Bicentenario de Ciencia y Tecnología de CONICYT" and "Programa Iniciativa Científica Milenio de MIDEPLAN"), with input from "Fondo de Innovación para la Competitividad, del Ministerio de Economía, Fomento y Turismo de Chile." J.A. and G.P. also acknowledge support by CONICYT through FONDECYT grants 3110142 and 11090421, respectively. Support for this research at Rutgers University was provided in part by NSF CAREER award AST-0847157 to S.W.J.

We thank all of the amateur astronomers who have searched for supernovae. The discovery of many SNe Iax is the result of their tireless effort. We especially thank C. Moore, discoverer of SN 2008ha. We gratefully acknowledge L. Bildsten, A. Gal-Yam, M. Hicken, D. Leonard, R. Margutti, T. Matheson, K. Moore, J. Nordin, L. Östman, H. Perets, T. Piro, E. Ramirez-Ruiz, D. Sahu, K. Shen, V. Stanishev, and S. Valenti for providing data, insights, and/or help for this study. R. Assef, A. Barth, V. Bennert, P. Berlind, P. Blanchard, G. Canalizo, B. Cenko, K. Clubb, D. Cohen, A. Diamond-Stanic, G. Folatelli, S. Hoenig, J. Irwin, M. Lazarova, N. Lee, A. Miller, A. Morgan, P. Nugent, D. Poznanski, J. Rex, A. Sonnenfeld, T. Steele, B. Tucker, and J. Walsh helped obtain some data presented in this paper; we thank them for their time. We are indebted to the staffs at the La Silla, Las Campanas, Lick, Keck, and Fred L. Whipple Observatories for their dedicated services.

Some of the data presented herein were obtained at the W. M. Keck Observatory, which is operated as a scientific partnership among the California Institute of Technology, the

University of California, and the National Aeronautics and Space Administration (NASA); the observatory was made possible by the generous financial support of the W. M. Keck Foundation. This research has made use of the NASA/IPAC Extragalactic Database (NED), which is operated by the Jet Propulsion Laboratory, California Institute of Technology, under contract with NASA. The analysis pipeline used to reduce the DEIMOS data was developed at UC Berkeley with support from NSF grant AST-0071048. NTT data was obtained under ESO Programme was 080.A-0516.

Part of the analysis occurred when R.J.F. visited the Aspen Center for Physics during the Summer 2012 workshops, "Non-Gaussianity as a Window to the Primordial Universe" and "The Evolution of Massive Stars and Progenitors of GRBs," as well as during his time at the Center as an independent researcher. This material is based upon work supported in part by the National Science Foundation under grant No. 1066293 and the hospitality of the Aspen Center for Physics. Some analysis was performed at the Woody Creek Community Center in Woody Creek, CO.

*Facilities:* Du Pont(Tek5), ESO:3.6m(EFOSC), FLWO:1.5m (FAST), Keck:I(LRIS), KAIT, Shane(Kast), Magellan:Baade (IMACS), Magellan:Clay(LDSS3), NTT(EMMI), CTIO: PROMPT, Swope(SITe3)

## REFERENCES

Abazajian, K. N., Adelman-McCarthy, J. K., Agüeros, M. A., et al. 2009, ApJS, 182, 543
Alard, C. 2000, A&AS, 144, 363
Alard, C., & Lupton, R. H. 1998, ApJ, 503, 325
Anderson, J., & Morrell, N. 2011, CBET, 2715, 2
Antilogus, P., Garavini, G., Gilles, S., et al. 2005, ATel, 502, 1
Arnett, W. D. 1982, ApJ, 253, 785
Barbon, R., Cappellaro, E., & Turatto, M. 1989, A&AS, 81, 421
Barentine, J., Bassett, B., Becker, A., et al. 2005, CBET, 268, 1
Bassett, B., Becker, A., Bizyaev, D., et al. 2007a, CBET, 1137, 1
Bassett, B., Becker, A., Brewington, H., et al. 2007b, CBET, 1057, 1
Benetti, S., Cappellaro, E., Mazzali, P. A., et al. 2005, ApJ, 623, 1011
Bessell, M. S., Schmidt, B. P., & Foley, R. J. 2010, CBET, 2337, 1
Bildsten, L., Shen, K. J., Weinberg, N. N., & Nelemans, G. 2007, ApJL, 662, L95
Blanchard, P., Cenko, S. B., Li, W., & Filippenko, A. V. 2011, CBET, 2678, 1
Blondin, S., & Berlind, P. 2008, CBET, 1198, 1
Blondin, S., & Calkins, M. 2008, CBET, 1250, 1
Blondin, S., Dessart, L., Leibundgut, B., et al. 2006, AJ, 131, 1648
Blondin, S., Matheson, T., Kirshner, R. P., et al. 2012, AJ, 143, 126
Blondin, S., & Tonry, J. L. 2007, ApJ, 666, 1024
Branch, D., Baron, E., Thomas, R. C., et al. 2004, PASP, 116, 903
Branch, D., Fisher, A., & Nugent, P. 1993, AJ, 106, 2383
Burket, J., & Li, W. 2005a, IAUC, 8625, 2
Burket, J., & Li, W. 2005b, IAUC, 8472, 1
Buzzoni, B., Delabre, B., Dekker, H., et al. 1984, Msngr, 38, 9
Cenko, S. B., Li, W., Filippenko, A. V., et al. 2012, CBET, 3014, 1
Chomiuk, L., Chornock, R., Soderberg, A. M., et al. 2011, ApJ, 743, 114
Chornock, R., Filippenko, A. V., Branch, D., et al. 2006, PASP, 118, 722
Contreras, C., Hamuy, M., Phillips, M. M., et al. 2010, AJ, 139, 519
Copin, Y., Gangler, E., Pereira, R., et al. 2012, ATel, 4476, 1
Dekker, H., Delabre, B., & Dodorico, S. 1986, Proc. SPIE, 627, 339
Dressler, A., Bigelow, B., Hare, T., et al. 2011, PASP, 123, 288
Fabricant, D., Cheimets, P., Caldwell, N., & Geary, J. 1998, PASP, 110, 79
Filippenko, A. V. 1997, ARA&A, 35, 309
Filippenko, A. V., & Chornock, R. 2003, IAUC, 8211, 2
Filippenko, A. V., & Foley, R. J. 2005, IAUC, 8486, 3
Filippenko, A. V., Foley, R. J., & Desroches, L. 2003, IAUC, 8170, 2
Filippenko, A. V., Foley, R. J., Silverman, J. M., et al. 2007a, CBET, 817, 1
Filippenko, A. V., Foley, R. J., Silverman, J. M., et al. 2007b, CBET, 926, 1
Filippenko, A. V., Li, W. D., Treffers, R. R., & Modjaz, M. 2001, in ASP Conf. Ser. 246: IAU Colloq. 183: Small Telescope Astronomy on Global Scales, ed. B. Paczynski, W.-P. Chen, & C. Lemme (San Francisco, CA: ASP), 121
Filippenko, A. V., Richmond, M. W., Branch, D., et al. 1992a, AJ, 104, 1543
Filippenko, A. V., Richmond, M. W., Matheson, T., et al. 1992b, ApJL, 384, L15
Fink, M., Röpke, F. K., Hillebrandt, W., et al. 2010, A&A, 514, A53
Folatelli, G., Phillips, M. M., Morrell, N., et al. 2012, ApJ, 745, 74
Foley, R. J. 2008, CBET, 1576, 2
Foley, R. J., Brown, P. J., Rest, A., et al. 2010a, ApJL, 708, L61
Foley, R. J., Challis, P. J., Filippenko, A. V., et al. 2012a, ApJ, 744, 38
Foley, R. J., Chornock, R., Filippenko, A. V., et al. 2009, AJ, 138, 376
Foley, R. J., & Filippenko, A. V. 2005, IAUC, 8465, 2
Foley, R. J., & Kasen, D. 2011, ApJ, 729, 55
Foley, R. J., Moore, M., Wong, D. S., Pooley, D., & Filippenko, A. V. 2006, CBET, 694, 1
Foley, R. J., Narayan, G., Challis, P. J., et al. 2010b, ApJ, 708, 1748
Foley, R. J., Papenkova, M. S., Swift, B. J., et al. 2003, PASP, 115, 1220
Foley, R. J., Rest, A., Stritzinger, M., et al. 2010c, AJ, 140, 1321
Foley, R. J., Sanders, N. E., & Kirshner, R. P. 2011, ApJ, 742, 89
Foley, R. J., Simon, J. D., Burns, C. R., et al. 2012b, ApJ, 752, 101
Gal-Yam, A. 2005, ATel, 391, 1
Gal-Yam, A., & Maoz, D. 1999, IAUC, 7130, 1
Gal-Yam, A., Maoz, D., Guhathakurta, P., & Filippenko, A. V. 2008, ApJ, 680, 550
Gal-Yam, A., Maoz, D., Stathakis, R. A., & Aldering, G. 2000, IAUC, 7357, 2
Gamezo, V. N., Khokhlov, A. M., Oran, E. S., Chtchelkanova, A. Y., & Rosenberg, R. O. 2003, Sci, 299, 77
Ganeshalingam, M., Li, W., & Filippenko, A. V. 2011, MNRAS, 416, 2607
Ganeshalingam, M., Li, W., Filippenko, A. V., et al. 2010, ApJS, 190, 418
Ganeshalingam, M., Li, W., Filippenko, A. V., et al. 2012, ApJ, 751, 142
Garavini, G., Folatelli, G., Goobar, A., et al. 2004, AJ, 128, 387
Geier, S., et al. 2012, arXiv:1209.4740
Gomez, G., Lopez, R., & Sanchez, F. 1996, AJ, 112, 2094
Graham, J., Weisz, D., Li, W., et al. 2003, IAUC, 8168, 1
Graur, O., Poznanski, D., Maoz, D., et al. 2011, MNRAS, 417, 916
Hachinger, S., Mazzali, P. A., Taubenberger, S., et al. 2012, MNRAS, 422, 70
Hamuy, M., Folatelli, G., Morrell, N. I., et al. 2006, PASP, 118, 2
Hatano, K., Branch, D., Fisher, A., Millard, J., & Baron, E. 1999, ApJS, 121, 233
Hicken, M., Challis, P., Jha, S., et al. 2009, ApJ, 700, 331
Hicken, M., Challis, P., Kirshner, R. P., et al. 2012, ApJS, 200, 12
Hicken, M., Garnavich, P. M., Prieto, J. L., et al. 2007, ApJL, 669, L17
Horne, K. 1986, PASP, 98, 609
Howell, D. A., Sullivan, M., Nugent, P. E., et al. 2006, Natur, 443, 308
Iben, I., Jr., & Tutukov, A. V. 1991, ApJ, 370, 615
Jha, S., Branch, D., Chornock, R., et al. 2006, AJ, 132, 189
Jordan, G. C., IV, Perets, H. B., Fisher, R. T., & van Rossum, D. R. 2012, ApJL, 761, L23
Kasliwal, M. M., Kulkarni, S. R., Gal-Yam, A., et al. 2012, ApJ, 755, 161
Kasliwal, M. M., Kulkarni, S. R., Gal-Yam, A., et al. 2010, ApJL, 723, L98
Kelly, B. C. 2007, ApJ, 665, 1489
Khokhlov, A. M. 1991, A&A, 245, 114
Kromer, M., et al. 2013, MNRAS, 429, 2287
Landolt, A. U. 1992, AJ, 104, 340
Lee, N., Li, W., Newton, J., & Puckett, T. 2007, CBET, 809, 1
Leibundgut, B., Kirshner, R. P., Phillips, M. M., et al. 1993, AJ, 105, 301
Li, W., Filippenko, A. V., Chornock, R., et al. 2003, PASP, 115, 453
Li, W., Filippenko, A. V., Gates, E., et al. 2001a, PASP, 113, 1178
Li, W., Filippenko, A. V., Treffers, R. R., et al. 2001b, ApJ, 546, 734
Li, W., Leaman, J., Chornock, R., et al. 2011, MNRAS, 412, 1441
Li, W., Singer, D., & Boles, T. 2004, IAUC, 8361, 1
Li, W. D., Filippenko, A. V., Treffers, R. R., et al. 2000, in AIP Conf. Proc. 522, Cosmic Explosions: Tenth Astrophysics Conference, ed. S. S. Holt & W. W. Zhang (Melville, NY: AIP), 103
Lira, P., Suntzeff, N. B., Phillips, M. M., et al. 1998, AJ, 115, 234
Livne, E. 1990, ApJL, 354, L53
Livne, E., & Arnett, D. 1995, ApJ, 452, 62
Maeda, K., Taubenberger, S., Sollerman, J., et al. 2010, ApJ, 708, 1703
Maund, J. R., Wheeler, J. C., Wang, L., et al. 2010, ApJ, 722, 1162
Maza, J., Hamuy, M., Antezana, R., et al. 2011, CBET, 2715, 1
Mazzali, P. A., Röpke, F. K., Benetti, S., & Hillebrandt, W. 2007, Sci, 315, 825
McClelland, C. M., Garnavich, P. M., Galbany, L., et al. 2010, ApJ, 720, 704
Miller, J. S., & Stone, R. P. S. 1993, Lick Obs. Tech. Rep. 66 (Santa Cruz: Lick Obs.)
Milne, P. A., Brown, P. J., Roming, P. W. A., et al. 2010, ApJ, 721, 1627
Minkowski, R. 1941, PASP, 53, 224
Monard, L. A. G. 2010, CBET, 2334, 1
Moriya, T., Tominaga, N., Tanaka, M., et al. 2010, ApJ, 719, 1445
Nakano, S., Ichimura, Y., Itagaki, K., Kadota, K., & Hirose, Y. 2008, CBET, 1193, 1
Narayan, G., Foley, R. J., Berger, E., et al. 2011, ApJL, 731, L11

Nomoto, K. 1982, ApJ, 257, 780
Oke, J. B., Cohen, J. G., Carr, M., et al. 1995, PASP, 107, 375
Östman, L., Nordin, J., Goobar, A., et al. 2011, A&A, 526, A28
Parrent, J. T., Thomas, R. C., Fesen, R. A., et al. 2011, ApJ, 732, 30
Pastorello, A., Smartt, S. J., Botticella, M. T., et al. 2010, ApJL, 724, L16
Perets, H. B., Gal-Yam, A., Mazzali, P. A., et al. 2010, Natur, 465, 322
Perna, R., Soria, R., Pooley, D., & Stella, L. 2008, MNRAS, 384, 1638
Phillips, M. M. 1993, ApJL, 413, L105
Phillips, M. M., Li, W., Frieman, J. A., et al. 2007, PASP, 119, 360
Phillips, M. M., Wells, L. A., Suntzeff, N. B., et al. 1992, AJ, 103, 1632
Pignata, G., Cifuentes, M., Maza, J., et al. 2010, CBET, 2184, 1
Pignata, G., Maza, J., Hamuy, M., et al. 2008, CBET, 1531, 1
Pignata, G., Maza, J., Hamuy, M., et al. 2009, CBET, 1661, 1
Pogge, R. W., Garnavich, P., & Pedani, M. 2011, CBET, 2678, 2
Pollas, C., Filippenko, A. V., Cappellaro, E., & della Valle, M. 1992, IAUC, 5420, 2
Poznanski, D., Chornock, R., Nugent, P. E., et al. 2010, Sci, 327, 58
Puckett, T., & Ireland, R. 2004, CBET, 102, 1
Puckett, T., & Langoussis, A. 2002, IAUC, 7847, 2
Puckett, T., Langoussis, A., & Harris, B. 2005, CBET, 154, 1
Puckett, T., Langoussis, A., & Marcus, M. 2003, CBET, 38, 1
Puckett, T., Moore, C., Newton, J., & Orff, T. 2008, CBET, 1567, 1
Quimby, R. M., Kulkarni, S. R., Kasliwal, M. M., et al. 2011, Natur, 474, 487
Quimby, R. M., Yuan, F., Akerlof, C., Wheeler, J. C., & Warren, M. S. 2012, AJ, 144, 177
Rajala, A. M., Fox, D. B., Gal-Yam, A., et al. 2005, PASP, 117, 132
Reichart, D., Nysewander, M., Moran, J., et al. 2005, NCimC, 28, 767
Rest, A., Narayan, G., Berger, E., et al. 2009, CBET, 2012, 1
Riess, A. G., Press, W. H., & Kirshner, R. P. 1996, ApJ, 473, 88
Ruiter, A. J., Belczynski, K., Sim, S. A., et al. 2011, MNRAS, 417, 408
Russell, B. R., & Immler, S. 2012, ApJL, 748, L29
Sahu, D. K., Tanaka, M., Anupama, G. C., et al. 2008, ApJ, 680, 580
Scalzo, R., Aldering, G., Antilogus, P., et al. 2012, ApJ, 757, 12
Sehgal, A., Gagliano, R., & Puckett, T. 2006, CBET, 653, 1
Shen, K. J., Kasen, D., Weinberg, N. N., Bildsten, L., & Scannapieco, E. 2010, ApJ, 715, 767
Silverman, J. M., & Filippenko, A. V. 2012, MNRAS, 425, 1917
Silverman, J. M., Filippenko, A. V., Barth, A. J., Walsh, J. L., & Assef, R. J. 2011a, CBET, 2681, 1
Silverman, J. M., Foley, R. J., Filippenko, A. V., et al. 2012, MNRAS, 425, 1789
Silverman, J. M., Ganeshalingam, M., Li, W., et al. 2011b, MNRAS, 410, 585
Sim, S. A., Fink, M., Kromer, M., et al. 2012, MNRAS, 420, 3003
Sostero, G., Puckett, T., & Orff, T. 2008, CBET, 1247, 1
Stanishev, V., Taubenberger, S., Blanc, G., et al. 2007, in AIP Conf. Proc. 924, The Multicolored Landscape of Compact Objects and Their Explosive Origins, ed. T. di Salvo, G. L. Israel, L. Piersant, L. Burderi, G. Matt, A. Tornambe, & M. T. Menna (Melville, NY: AIP), 336
Stritzinger, M. 2009, CBET, 1665, 1
Stritzinger, M., Folatelli, G., Pignata, G., & Phillips, M. M. 2010a, CBET, 2184, 2
Stritzinger, M., Leibundgut, B., Walch, S., & Contardo, G. 2006, A&A, 450, 241
Stritzinger, M., Phillips, M. M., Folatelli, G., & Foley, R. J. 2010b, CBET, 2191, 1
Stritzinger, M., Taddia, F., Fransson, C., et al. 2012, ApJ, 756, 173
Stritzinger, M. D., Phillips, M. M., Boldt, L. N., et al. 2011, AJ, 142, 156
Sullivan, M., Kasliwal, M. M., Nugent, P. E., et al. 2011, ApJ, 732, 118
Tanaka, M., Kawabata, K. S., Yamanaka, M., et al. 2010, ApJ, 714, 1209
Tanaka, M., Mazzali, P. A., Stanishev, V., et al. 2011, MNRAS, 410, 1725
Thomas, R. C., Aldering, G., Antilogus, P., et al. 2011, ApJ, 743, 27
Townsley, D. M., Moore, K., & Bildsten, L. 2012, ApJ, 755, 4
Travaglio, C., Hillebrandt, W., Reinecke, M., & Thielemann, F.-K. 2004, A&A, 425, 1029
Tutukov, A., & Yungelson, L. 1996, MNRAS, 280, 1035
Valenti, S., Pastorello, A., Cappellaro, E., et al. 2009, Natur, 459, 674
Vennes, S., Kawka, A., O'Toole, S. J., Németh, P., & Burton, D. 2012, ApJL, 759, L25
Wade, R. A., & Horne, K. 1988, ApJ, 324, 411
Waldman, R., Sauer, D., Livne, E., et al. 2011, ApJ, 738, 21
Wood-Vasey, W. M., Aldering, G., Nugent, P., et al. 2002, IAUC, 7902, 3
Woosley, S. E., & Kasen, D. 2011, ApJ, 734, 38
Woosley, S. E., & Weaver, T. A. 1994, ApJ, 423, 371
Wright, D., Chen, T.-W., Fraser, M., et al. 2012, ATel, 4516, 1
Yamanaka, M., Kawabata, K. S., Kinugasa, K., et al. 2009, ApJL, 707, L118